Late Quaternary vegetation and climate dynamics in central-eastern Brazil: insights from a ~35k cal a BP peat record in the Cerrado biome

Short running title: **Late Quaternary vegetation and climate in central-eastern Brazil**

INGRID HORÁK-TERRA[1*], ANTONIO MARTÍNEZ CORTIZAS[2], CYNTHIA FERNANDES PINTO DA LUZ[3], ALEXANDRE CHRISTÓFARO SILVA[4], TIM MIGHALL[5], PLÍNIO BARBOSA DE CAMARGO[6], CARLOS VICTOR MENDONÇA-FILHO[7], PAULO EDUARDO DE OLIVEIRA[8], FRANCISCO WILLIAN CRUZ[8], PABLO VIDAL-TORRADO[9]

[1]Instituto de Ciências Agrárias, Universidade Federal dos Vales do Jequitinhonha e Mucuri – ICA/UFVJM, BR 251 Av. Universitária, 1000, Universitários, 38610000, Unaí, MG, Brazil; ingrid.horak@ufvjm.edu.br.

[2]Eco-Past (GI-1553), Faculty of Biology, Universidade de Santiago de Compostela - USC, Santiago de Compostela, 15782, Spain; antonio.martinez.cortizas@usc.es.

[3]Núcleo de Pesquisa em Palinologia, Instituto de Botânica, Secretária de Infraestrutura e Meio Ambiente do Estado de São Paulo – IBt/SP, São Paulo, SP, 04301902, Brazil; cyluz@yahoo.com.br.

[4]Departamento de Engenharia Florestal, Universidade Federal dos Vales do Jequitinhonha e Mucuri - UFVJM, Diamantina, MG, 39100000, Brazil; alexandre.christo@ufvjm.edu.br.

[5]School of Geosciences, University of Aberdeen, Aberdeen, G22 St Mary's, UK; t.mighall@abdn.ac.uk.

[6]Laboratório de Ecologia Isotópica, Centro de Energia Nuclear na Agricultura - CENA/USP, Piracicaba, SP, 13416-903, Brazil; pcamargo@cena.usp.br.

[7]Departamento de Ciências Biológicas, Universidade Federal dos Vales do Jequitinhonha e Mucuri - UFVJM, Diamantina, MG, 39100000, Brazil; cvmendonca@gmail.com.

[8]Departamento de Geologia Sedimentar e Ambiental, Instituto de Geociências – IGc/USP, São Paulo, SP, 05508-080, Brazil; paulo.deoliveira@usp.br; cbill@usp.br.

[9]Departamento de Ciência do Solo, Escola Superior de Agricultura "Luiz de Queiroz" – ESALQ/USP, Piracicaba, SP, 13418900, Brazil; pvidal@usp.br.

*Corresponding author. Instituto de Ciências Agrárias, Universidade Federal dos Vales do Jequitinhonha e Mucuri – ICA/UFVJM, BR 251 Av. Universitária, 1000, Universitários, 38610000, Unaí, MG, Brazil, E-mail addresses: ingrid.horak@ufvjm.edu.br, ingridhorak@yahoo.com.br (I. Horák-Terra).

ABSTRACT: The late Quaternary evolution of central-eastern Brazil has been under-researched. Questions remain as to the origin of the Cerrado, a highly endangered biome, and other types of vegetation, such as the Capões – small vegetation islands of semi-deciduous and mountain forests. We investigated the factors that influenced the expansion and contraction of the Cerrado and Capões during the late Quaternary (last ~35 ka), using a multi-proxy approach: stable isotopes ($\delta^{13}C$, $\delta^{15}N$), geochemistry, pollen, and multivariate statistics derived from a peat core (Pinheiro mire, Serra do Espinhaço Meridional). Five major shifts in precipitation, temperature, vegetation and landscape stability occurred at different timescales. Our study revealed that changes in the South Atlantic Convergence Zone (SACZ) seem to have been coeval with these shifts: from late glacial maximum to mid-Holocene the SACZ remained stationed near (~29.6 to ~16.5k cal a BP) and over (~16.5 to ~6.1k cal a BP) the study area, providing humidity to the region. This challenges previous research which suggested that climate was drier for this time period. At present, the Capões are likely to be a remnant of a more humid climate; meanwhile, the Cerrado biome seems to have stablished in the late Holocene, after ~3.1k cal a BP.

KEYWORDS: Paleoclimatology; Stable isotopes; Pollen; Geochemistry; Peatlands.

Introduction

Central-eastern Brazil, with a sub-humid and seasonal climate and well-defined seasons (~4-5 months of dry season and mean winter temperature ≥ 15°C), maintains the Cerrado biome, which is a vast tropical savanna and part of the so-called "xeric vegetation" corridor (Bucher, 1982). This tropical savanna is characterized by large diversity of phytophysiognomies and high levels of

endemism, and quite specific vegetation patterns are found in certain regions, such as the Serra do Espinhaço Meridional (Minas Gerais state). Here small vegetation islands, called "Capões" (also "florestas em mancha" by Rizzini, 1979), are characterized by tree and shrub species of semi-deciduous forest (with double climatic seasonality) and mountain forests (mean winter temperature < 10°C; Ledru, 1993) dispersed among grassland formations.

The response of tropical biomes to climate change has been the focus of investigations covering the last glacial maximum (LGM; peaked 21.5 ka) and mid-Holocene (MH; 5 ka) (Colinvaux *et al*., 1996; Ledru *et al*., 2009; Bueno *et al*., 2016; Arruda *et al*., 2017; Pinaya *et al*., 2019). However, none of them were performed in the Cerrado biome, specifically in the Serra do Espinhaço Meridional. Therefore, palaeorecords and Pleistocene reconstructions are absent from this area and this is one of the main reasons for undertaking this study. Several earlier studies have challenged established hypotheses, such as Amazonian refugia (Haffer, 1969) and Pleistocene arc hypotheses (Prado and Gibbs, 1993), which assert that aridity was prevalent in the Cerrado biome during these periods. More recent research has questioned this interpretation, stating that the humid forest of the Amazon region was already present in the LGM (Colinvaux *et al*., 1996; Haberle and Maslin, 1999; Leite *et al*., 2016; Arruda *et al*., 2017). Additionally, the spatial distribution of seasonal biomes was larger during the Holocene compared to the LGM, helped by improved recent climatic conditions (Werneck *et al*., 2011; Horák-Terra *et al*., 2015).

It has been proposed that the advance of Quaternary glaciers in temperate regions (the last glacial period encompassed the period 115–11.7 ka) resulted in the development of xerophile vegetation, such as savannas in tropical and subtropical areas (Goldblatt, 1978; Pennington *et al*., 2006), but it is not clear whether this is a typical vegetation response to changing climate. Currently, the distribution of these complex Neotropical plant communities – the actual Cerrado – contradicts this proposal, since a vast dense forest should cover the approximately 2 million km^2 of

74 the Brazilian territory if this idea was true. Similarly, there are other unsolved questions such as: are
75 the present occurrence of Capões relicts of a more dense arboreal vegetation of former times?; was
76 there a more arid climate in the past, and was its vegetational composition similar to the current
77 one?; and was there a time when the area now occupied by the Cerrado served as ecotone of the
78 wettest biomes?

79 Precise characterization of climate variability in the Cerrado biome on a wide range of
80 timescales is necessary to understand its possible link to the establishment of tropical biomes in
81 South America (Simon *et al*., 2009; Werneck *et al*., 2012), since it is bordered by almost all other
82 biomes today. However, paleoclimate data of central-eastern Brazil are still scarce (Ferraz-Vicentini
83 and Salgado-Labouriau, 1996; Barberi *et al*., 2000; Stríkis *et al*., 2011; Horák-Terra *et al*., 2015).
84 Therefore, it is unclear how millennial and orbital-scale climate variability manifested itself in this
85 area and how it compares with adjacent regions.

86 Supported by the interhemispheric anti-phase behavior, the Younger Dryas (YD)-Heinrich
87 (H) and the Dansgaard-Oeschger (D/O) events respectively expressed in South America as wet and
88 dry episodes (Cheng *et al*., 2013). The YD occurred by 12.9-11.7 ka, while the H and D/O were
89 characterized by a series of events (10 and 25 events respectively) during the last glacial period.
90 The abrupt increase in monsoon rainfall during the YD-H events was likely related to a southward
91 shift in the average position of the Intertropical Convergence Zone (ITCZ), a strengthening of the
92 asymmetry in Hadley circulation in response to an interhemispheric gradient of sea surface
93 temperature, and a possible influence of Antarctic climate changes (Wang *et al*., 2004, 2006;
94 Kanner *et al*., 2012; Cheng *et al*., 2013). Despite this coherent pattern of millennial-scale
95 variability, the spatial structure of precipitation is complex at orbital timescales (Wang *et al*., 2006).
96 For instance, it is known that northeastern Brazil experienced humid conditions during low summer
97 insolation phases and aridity conditions when summer insolation was high, whereas the rest of
98 southern tropical South America showed an opposite behavior (Cheng *et al*., 2013). Thus, obtaining

accurate information about the past climate of central-eastern Brazil is important, mainly due to its strategic location. This region is deeply influenced by the South Atlantic convergence zone (SACZ) during the austral summer, resulting in increasing precipitation from November to March (Garreaud *et al*., 2009), when it extends into a southeastern direction from the interior of the continent to the South Atlantic (Vera *et al*., 2006).

Tropical and subtropical peatlands are ideal archives for reconstructing climate changes from the late Pleistocene – i.e. from 126 ka (Weiss *et al*., 2002; Muller *et al*., 2008; Ledru *et al*., 2009; Dommain *et al*., 2011; Swindles *et al*., 2018), since they are extremely sensitive to changes in hydrology. For example, Horák-Terra *et al*. (2015) investigated a peat core from Pau de Fruta mire, located in the Serra do Espinhaço Meridional (Brazil), using a combination of biotic (pollen) and abiotic (peat physical properties, elemental and isotopic composition) proxies to trace Holocene climate changes in the area. Morphological, physical, chemical, and elemental properties were used to show that the peatland showed a complex evolution resulting from varying mineral fluxes from the catchment, regional dust deposition, changes in peat plant communities and degree of peat decomposition (Horák-Terra *et al*., 2014). Similarly, we present results from a core (PI, 130 cm deep) spanning the last ~35k cal a BP, and taken from a tropical mountain peatland (Pinheiro mire) from Serra do Espinhaço Meridional. The same core was also investigated for mercury (Pérez-Rodríguez *et al*., 2015, 2016). This research showed that variations in Hg concentrations were most likely driven by climate, either indirectly by enhancing the mineral matter fluxes from the mire's catchment (i.e. increased soil erosion) and regional dust deposition, or directly by long-term changes in atmospheric wet deposition (humid vs arid phases). So, this core presents a unique opportunity for a detailed investigation to reconstruct climate change in central-eastern Brazil since the late Pleistocene, taking into account the existence of autogenic changes in Pinheiro mire by multiple mechanisms as cited above.

We present inferences about past environmental conditions in central-eastern Brazil during the ~35k cal a BP using a multi-proxy data including stable isotopes ($\delta^{13}C$, $\delta^{15}N$), geochemistry (major, minor, and trace elements), and pollen records (pollen, spores, and other non-pollen palynomorphs). From these data, reconstructions of changes in precipitation, temperature, vegetation, and landscape stability occurring at different timescales allowed us to achieve our main aims: (1) to obtain accurate information about the past climate of central-eastern Brazil, and (2) to reconstruct the vegetation history and the conditions culminating in the formation of the current biome. Our study is one of the most complete for central-eastern Brazil. The data can also be used to predict future conditions through climate models, as well as for comparing with other paleoclimatic and paleoecological records from different regions in Brazil and globally. Furthermore, our research highlights the value of such data for conservation of tropical peatlands and Cerrado biome, due to their environmental and ecological importance.

Materials and methods

Regional setting

The PI core was collected from the Pinheiro mire (18°3'44.42" S 43°39'42.37" W), a tropical mountain peatland located at ~1240 m a.s.l. in the Serra do Espinhaço Meridional, Minas Gerais state (Brazil) (Fig. 1 and Figs. 2A and 2B). Pinheiro is an oligotrophic valley mire located in a catchment with limited drainage. The catchment is narrow (0.1 to 0.6 km wide) and elongated (~3.7 km long) in a SW-NE direction, and the mire covers the lower and flatter parts of the valley overlaying quartzitic sediments. The Pinheiro mire is also a soligeneous peatland: it is affected by water from external sources percolating through or over surface peat. Today, the peat is mostly formed by graminoid species, among them grasses and sedges. The basal lithology is part of the Galho do Miguel formation, constituted by pure and thin quartzites (~90%), thin micaceous quartzites and some gray or greenish metargilites (~5 a 10%; Knauer, 2007).

147 At present, the climate of the area is tropical montane with mean annual temperature of 18.7
148 °C and mean annual precipitation about 1500 mm - period 1950 to 1990 (Alves et al., 2013),
149 restricted by the South American Monsoon System (SAMS) activity and SACZ.

150 The vegetation is typical of the Cerrado biome (Brazilian savanna), one of the most
151 endangered in the world (Klink and Machado, 2005). This is characterised by extensive, open
152 grasslands (wet, dry, and rupicola-saxicolous), with a limited presence of trees and shrubs.
153 However, it also contains the "Capões" (with semi-deciduous forest and mountain forest species),
154 which appear as small, dispersed forest islands (Figs. 2A and 2B). Currently, the Pinheiro area is
155 quite well preserved, since access for the locals living in the surrounding villages is difficult.
156 However, there are reports of some natural bushfires during the driest times of the year.

157 ***Sampling and stratigraphic description***

158 The core was sampled in 2010 using a vibracore (constructed according to Martin *et al.*,
159 1995) to a depth 324 cm. However, as this paper mainly deals with changes in environment and
160 climate for the LGM - mid-Holocene, we have decided to only present the upper 130 cm, which
161 span the last ~35ka. The stratigraphy was described according to the Field Book for Describing and
162 Sampling Soils (Schoeneberger *et al.*, 1998) and the Guidelines for Soil Description (FAO, 2006),
163 whereas the horizons were defined according to the Soil Taxonomy (Soil Survey Staff, 2010). The
164 upper 130 cm is composed of 5 peat horizons (Oi, Oa, Oa2, Oa3, and Oa4), defined by the content
165 of mineral/organic matter, the degree of peat decomposition, and consistency (Fig. 2C): horizons
166 Oa4 (130-98 cm) and Oa3 (98-58 cm) are slightly sticky and with low mineral matter content,
167 differing only in fine roots content (greater in Oa4 than in Oa3); horizons Oa2 (58-20 cm) and Oa
168 (20-8 cm) are also similar, both with abundant fine roots and highly sticky; and the uppermost layer,
169 Oi (8-0 cm), is a fibric horizon of poorly decomposed peat. The core was sliced into continuous 2
170 cm-thick sections.

171 ***Age-depth model of the core***

172 Seven peat samples (Supplementary Table S1) were radiocarbon dated by AMS in Beta
173 Analytic Inc. (Miami, USA); the analyses were done on the acid-alkaline-acid extraction of bulk
174 organic matter. The age-depth model was fitted with a Bayesian statistical approach using the
175 Bacon R package (v.2.3.5) (Blaauw and Christen, 2011) (Figure 3). The calibration curve was
176 SHCal13.14C (Hogg *et al*., 2013). Based on the hypothesis that Northern Hemisphere air masses
177 may have been the main source of humidity for the area in the late Quaternary, we also performed
178 the age model using the NH calibration data set (IntCal13; Supporting Fig. S1). Since the results
179 indicated that the models are in close agreement, with very close ages, we present the chronologies
180 with the model obtained with the Southern Hemisphere calibration curve here. The model was fitted
181 by assigning the year of sampling as age of the upper peat sample and no smoothing was applied.
182 All ages presented in the text are expressed as calibrated ages.

183 ***Elemental and isotopic composition***

184 Carbon and nitrogen contents and isotopic composition - $\delta^{13}C$ and $\delta^{15}N$ - were determined in
185 dried, milled, and homogenized peat samples, using an elemental analyzer coupled to a mass
186 spectrometer hosted in the Laboratório de Ecologia Isotópica of the Centro de Energia Nuclear na
187 Agricultura - CENA/USP (Piracicaba, SP, Brazil). Major, minor and trace elements (P, S, Al, Si,
188 Fe, Ti, K, Ca, Ga, Rb, Sr, Y, Zr, Nb, Th, Cr, Mn, Ni, Cu, Zn, As, Pb, Cl, and Br) were determined
189 by X-ray fluorescence in the same samples using two energy dispersive XRF analyzers (Cheburkin
190 and Shotyk, 1996; Weiss *et al*., 1998) hosted in the RIAIDT facility (Infrastructure Network for the
191 Support of Research and Technological Development) of the Universidade de Santiago de
192 Compostela (Spain).

193 Instrument calibrations were performed for organic matrices using several reference
194 materials (NIST 1515, 1541, 1547, and 1575; BCR 60 and 62; and V-1). Detection limits were:

195 <100 μg g^{-1} for Al, Si, S, K, Ca, and Fe; 50 μg g^{-1} for P; 10 μg g^{-1} for Mn; 5 μg g^{-1} for Ti; 10 μg g^{-1}
196 for Cl; 1 μg·g^{-1} for Cr, Ni, Cu, Zn, Br, Ga, Rb, Sr, As, Y, Zr, Th, Pb, and Nb. One in every five
197 samples was analyzed in triplicate, and the measurements agreed within a 5% for most elements.
198 Values that did not agree within 10% were rejected (in this case, more replicates were done).

199 ***Pollen study***

200 For the pollen study, 13 wet samples of 1 cm in thickness taken every 10 cm were obtained
201 from the center of the PI core. A modified version of the physico-chemical treatment (Ybert *et al.*
202 1992) extracted pollen, spores, and other non-pollen palynomorphs (NPP). Hydrofluoric acid was
203 added for the dissolution of silicates, hydrochloric acid for elimination of fluorosilicates, acetic acid
204 for dehydration and acetolysis mixture for dissolution of the organic matter and acetylation of the
205 exine. Ultrasound was used to separate large organic remains. The counting was undertaken at 400
206 X under microscope (Supplementary Table S2), obtaining an average total land pollen sum (TLP)
207 of 800 terrestrial pollen grains per sample. Hydro-hygrophytes and NPP were not included in the
208 TLP, but they were expressed as percentages of it. The average sum of hydro-hygrophytes and NPP
209 was 560 palynomorphs. Identification was helped by the reference collection (modern pollen
210 deposition) of the Pau de Fruta mire (Horák, 2009; Horák *et al.*, 2015; Luz *et al.*, 2017),
211 identification keys, and atlases (van Geel, 1978; Tryon and Tryon, 1982; Roubik and Moreno,
212 1991). Taxa included in the TLP are considered indicators of regional vegetation, while hydro-
213 hygrophytes and NPP are mainly considered to constitute a local signal. The NPP can be mostly
214 considered as local indicators since their dispersal is limited (Salgado-Labouriau, 2007); however,
215 the case of the hydro-hygrophyte taxa, e.g. Cyperaceae, is more complex, as they could also be part
216 of the regional communities (Horák-Terra *et al.*, 2015). Pinheiro is a valley mire and variations in
217 the water table depth could be responsible for differences in the spatial distribution of local plant
218 communities. For this reason, we added the hydro-hygrophytes in the local signal. Pollen diagrams
219 were obtained in the R software using Rioja package (Juggins, 2019).

Groups corresponding to the types of vegetation and environments were obtained (Fig. 5) and based on the ecological preferences of the identified taxa (Figs. 6 and 7, Supporting Figs. S8, S9, S10, and S11). The knowledge of each taxa is based on the detailed botanical survey of the Pinheiro mire and of other peatlands from the region (all materials are cataloged in the DIAM Herbarium of the Universidade Federal dos Vales do Jequitinhonha e Mucuri - UFVJM, Diamantina city, Minas Gerais state, Brazil), but also used several other references when necessary (van Geel, 1978; Guy-Ohlson, 1992; Mendonça *et al*., 1998; Marchant *et al*., 2002; Luz *et al*., 2017). The Supplementary Table S3 contains all identified taxa and their respective habit and coverage regional or local information, as well as indicating their phytophysiognomy or preferred environmental conditions. We are aware that some taxa can only be identified at the family or genera level and may include plants from various habitats, and also that most taxa identified at the species level may not be exclusive of one habitat and cannot be associated exclusively to one type of vegetation or environment. We also take into account the concept of "non-analogous community" and, therefore we assume that plant communities are not fixed through time (Williams and Jackson, 2007; Keith *et al*., 2009), and that species respond individualistically to climate change. So, the floristic composition of vegetation changed through time, probably occurring a certain dynamic (or, a rearrangement) of the different taxa within each group.

Information about the length of the dry season for the main vegetation types from south to north Brazil was obtained to support climate inferences (Ledru *et al*., 1998). For vegetation typical of drier climate (Cerrado encompassing savanna forest and dry grassland), 5-6 months of dry season was considered. For seasonal forests (mainly semi-deciduous forest), 2-3 months of dry season was considered. And, finally, no dry season was considered for mountain forest (encompassing cold and humid forest).

Statistical analysis

Stratigraphically constrained cluster analysis (total sum of squares method; Grimm, 1987) was applied to pollen and NPP/hydro-hygrophyte data to define regional and local palynological zones, using the broken stick model to find the appropriate number of zones. For geochemical data, principal component analysis (PCA) was performed on the data matrices (these data can be seen in Supporting Figs. S3-S7) after log-transformation and standardization (as suggested for compositional data, i.e., close data sets; Reimann *et al*., 2008) in correlation mode and applying a varimax rotation to maximize the variable loadings in the components (Eriksson *et al*., 1999). PCA was performed using SPSS 20.0 software.

Supporting studies

The $\delta^{18}O$ curve from a Greenland ice record (Grootes and Stuiver, 1997) was included in this study, showing the typical sequence of stadial (YD + H1 to H3, at the top of the Fig. 4B) and interstadial (D/O cycles, from 1 to 7 at the bottom of the Fig. 4B) periods. For comparison, $\delta^{18}O$ records of speleothems from northeastern (Cruz *et al*., 2009; Fig. 4C) and southern Brazil (Cruz *et al*., 2005; Fig. 4D) and western Amazonia (Cheng *et al*., 2013; Fig. 4E) are also included, as well as the Austral summer insolation (ASI) curve (Berger, 1978; in red). The oxygen isotope ratios are mainly interpreted as a function of the isotopic composition of rainfall, therefore as indicative of past precipitation, where more negative $\delta^{18}O$ values are associated with intense SAMS regime (Wang *et al*., 2004, 2006) or wet climate conditions (Cheng *et al*., 2013). The ASI can be used to examine the impact of orbital forcing, defined as the combined effects of precession and eccentricity (Berger, 1978) on central-eastern Brazilian climate. Changes in Earth's orbit around the sun cause quasi-periodic changes in insolation reaching the top of the atmosphere (Liu and Battisti, 2015).

Results

Proxies: meaning and interpretation

The age-depth model obtained for PI core provides a chronology for the last ~35k cal a BP of environmental changes in central eastern Brazil (Figure 3). We are aware of the limitation imposed by such a coarse dating resolution for the covered period, and the larger uncertainty introduced by extrapolating ages for the last 30 cm (older than ~26ka). This extrapolation is necessary because we have data for almost all proxies in this secction, so it seems recommendable to indicate the expected ages for the observed changes. We emphasize that this strategy is widely used in Quaternary studies (De Oliveira et al., 2019; Rodríguez-Zorro et al., 2020).

We use a selection of proxies (Fig. 4), such as $\delta^{13}C$, $\delta^{15}N$, Cp2 (factor scores of the second PCA component on geochemical properties - Supporting Fig. S2), and the Br/C ratio, as well as information about distribution of the main taxa by type of vegetation and environment inferred by pollen analysis (Fig. 5; we have not included those taxa considered as ubiquitous). Synthetic pollen diagrams for the regional and local taxa are shown in Fig. 6 and Fig.7 respectively, while the remaining taxa not included in these figures can be found in Supporting Figs. S8 and S9. Factor loadings of the extracted components and the fractionation of communalities of the variables used in the PCA of the geochemical properties are provided in Supporting Fig. S3. Depth records of physical properties and elemental-isotopic composition of C and N (Supporting Fig. S4), major and minor elements (Supporting Fig. S5), trace lithogenic elements (Supporting Fig. S6), and trace metallic elements and halogens (Supporting Fig. S7) also used in the PCA are in the Supporting Information.

The $\delta^{13}C$ values can be used to identify carbon derived from different photosynthetic pathways, since the isotopic ratio does not change with time (Cerling *et al.*, 1989). This ratio also provides information about source vegetation and climate dynamics, because C_3 plants (most trees and some graminoids of wet grasslands and indicators of humid environments) have $\delta^{13}C$ values between -32 and -22‰, while C_4 plants (graminoids of dry environments) have ratios between -17 and -9‰ (O'Leary, 1988; Boutton, 1991). We might expect an 'in phase' trend when humidity

293 increases, directly related by $\delta^{13}C$, in agreement with the increase in ASI, and an "antiphase" when
294 the increase in humidity is not directly related to the ASI.

295 The main factors affecting the $\delta^{15}N$ ratio are: (i) the constant addition of organic matter
296 from plants in the upper soil layers and (ii) transformations of organic-N to inorganic-N, and among
297 inorganic-N forms. With increased mineralization, the remaining organic matter becomes enriched
298 in ^{15}N (Schellekens *et al*., 2014). In general, these processes occur during drier periods. In tropical
299 soils, the values vary between +3.5 and +21.7‰, with much smaller variations in hydromorphic
300 soils (between ≈+4 and +5‰) (Martinelli *et al*., 2009).

301 The second PCA component (Cp2) based on geochemical properties is characterized by
302 positive loadings of C, N, S (biophilic elements) and Br (organically bound element), and negative
303 loadings of Si, Cr, and K (lithogenic elements) (Supporting Fig. S2). Since the main geological
304 material of the catchment of the mire is quartzite, Si content is most probably related to the amount
305 of quartz transported from the catchment soils into the mire. Thus, Cp2 likely reflects a local signal:
306 the mire accumulates organic matter (positive factor scores) under stable conditions in the
307 catchment, while larger amounts of coarse mineral matter (i.e. quartz from the quartzite) are
308 transported to the mire (negative factor scores) under unstable conditions (erosion episodes).

309 The oceans are the main source of Br, which reaches the peatland by wet deposition and
310 accumulates as organo-halogenated compounds (Biester *et al*., 2006). Given the inland location of
311 the Pinheiro mire, Br deposition may have been linked to atmospheric circulations bringing sea-
312 spray and precipitation (Lalor, 1995). The Br/C ratio is used here to reflect the excess of Br that
313 cannot be explained by a substrate effect (i.e. availability of organic matter for bromination) and
314 thus infers changes in rainfall.

315 ***The chronology of environmental changes***

316 ***Marine Isotope Stage 3 (MIS 3)***

317 Although our record only shows the end of the MIS 3, a cold phase in the Northern
318 Hemisphere, it is noteworthy that a change in the climate pattern occurs from the first half (~35.0 to
319 ~31.8k cal a BP) to the second half (~31.8 to ~29.6k cal a BP) and before the LGM. There was no
320 speleothem deposition (formation) in caves in northeastern Brazil during MIS 3 (Fig. 4C; Wang *et*
321 *al*., 2004; Cruz *et al*., 2009). The D/O 7, 6, and 5 cycles (~34.6, ~32.9, and ~31.7k cal a BP
322 respectively) correspond to high $\delta^{13}C$ values in our record, indicating that long dry seasons (5 or
323 more months) were particularly recurrent, as corroborated by high peat mineralization (high $\delta^{15}N$
324 values; Fig. 4A2). High levels of erosion from catchment soils (negative Cp2 values; Fig. 4A3)
325 were probably triggered and facilitated by the reduction of seasonal forests (see for example
326 *Cedrela*, *Celtis*, *Sorocea*, *Trema*, *Hyeronima*, and Myrtaceae) and expansion of pioneer trees
327 (*Cecropia*) (Figs. 5 and 6), which reduced soil protection. Given these fluctuations, a dry climate is
328 evident for the MIS 3 in central-eastern Brazil, much drier in the first phase. However, climate was
329 warm overall (*Byrsonima* and *Smilax*; representative of savanna) with some inter-dispersed cooling
330 events (*Cedrela*, *Myrsine, Podocarpus*, and *Weinmannia* taxa; all indicators of tropical coniferous
331 forest related to mountainous and cold conditions), which are synchronous with the milder climate -
332 relative short increases in humidity (as seen by fluctuating of the already mentioned taxa of
333 seasonal forest), but still within a dry season (from 2 to 3 months, lasting less than 1,000 years).

334 ***Last Glacial Maximum - mid-Holocene***

335 With the onset of the LGM by ~29.6k cal a BP, a new pattern of climate conditions was
336 established and remained until the early mid-Holocene (~6.1k cal a BP). Predominantly wet
337 conditions are supported by the almost constant low $\delta^{13}C$ values (more negatives than in MIS 3;
338 Fig. 4A1) and by the return of seasonal forest and expansion of cold and humid forest (mainly
339 represented by *Podocarpus*), as indicated by pollen data (Fig. 6) for H2, H1, and YD at ~25.3,
340 ~15.8, and ~12.4k cal a BP, respectively, and beyond the ~8.2k cal a BP event. Catchment soil
341 erosion increased with increasing humidity (Fig. 4A3), but it was relatively lower than during MIS

342 3, most probably due to the denser tree-shrub vegetation cover (increasing trend of $\delta^{15}N$ values see-
343 saw pattern suggesting a greater accumulation of organic material; Fig. 4A2). From ~29.6 to ~17.0k
344 cal a BP, the increased humidity is simultaneous with an increase in southern Brazil and a decrease
345 in northeastern from ~26 to ~17.0k cal a BP. From ~16.0 to ~7.1k cal a BP, after the abrupt event of
346 dry (*Amaranthus*, *Borreria*, and *Gleichenia*; indicators of dry grassland) and very cold (highest
347 percentage of *Drimys* and presence of *Araucaria,* both are tropical coniferous) conditions by ~16.4k
348 cal BP, humid conditions returned when humidity also increased in the northeast and decreased in
349 the south as well as in western Amazonia (Figs. 4C, D, E). The Bølling-Allerød interstadial is
350 coeval with the D/O 1 cycle and is registered as a slight reduction of precipitation by ~14.3k cal BP,
351 which coincides with an absence of speleothem deposition in northeastern Brazil (Fig. 4C) and wet
352 climate in the south (Fig. 4D). In that last phase, high oceanic-atmospheric activity with the highest
353 Br/C ratios culminating by ~8.2k cal BP (Fig. 4A4) provide evidence of the probably wettest period
354 of the record, which is in agreement with records from northeastern Brazil (Fig. 4C).

355 ***Mid to Late Holocene***

356 After ~6.1k cal a BP, periods of torrential rainfall probably started amid the driest (long dry
357 season of ~6 months) and warm regional climate. Up until ~3.1k cal a BP, seasonal, cold and
358 humid- and mountain- forests retracted as dry grassland expanded (for example, *Amaranthus* and
359 *Borreria*; Fig. 6) and point to a decrease in humidity, while an almost constant presence of wet
360 grassland (*Drosera*, *Sagittaria*, *Utricullaria*, HdV-18 van Geel; Fig. 7) suggests local (i.e. in the
361 mire catchment) humid conditions. However, more seasonally distributed rainfall may have been
362 abundant enough to create bodies of stagnant water on the Pinheiro mire (highest percentage of
363 shallow open water indicators, such as *Mougeotia* and *Zygnema*; Figs. 5 and 7), similar to a shallow
364 lake and populated with species of wet grassland (C3 plants; Fig. 4). An abrupt reduction of
365 oceanic-atmospheric activity suggested by the Br/C ratios (Fig. 4A4), like that observed during MIS
366 3, supports the interpretation of prevailing dry climatic conditions. In this period, humidity also

decreased in the northeast while an opposite trend is seen for southern Brazil and western Amazonia (Figs. 4C, D, E).

An abrupt change in $\delta^{13}C$ occurred again after ~3.1k cal a BP, reaching its maximum value by AD ~740 (Fig. 4A1). The isotope ratios are comparable to those observed during MIS 3 and, together with indications of a decline in wet grasslands (Araceae, Cyperaceae, *Drosera*, *Typha*, *Utricullaria,* and diverse NPPs such as *Meliola niessleana*; Fig. 7), a slight increase in dry grassland (*Amaranthus*, *Borreria*, *Gleichenia*, *Gelasinospora*, *Pleospora*; Figs. 6 and 7), and increase in organic matter mineralization (Fig. 4A2), provide evidence of a decrease in local humidity. At regional scale, the small increase in the seasonal, mountain and pioneer trees – with typical taxa of the conditions mentioned above (Fig. 6) – indicates a relative increase in humidity. However, this period was probably warmer, as suggested by the expansion and stabilization of the savanna forest (Fig. 5), represented mainly by *Byrsonima*, *Tabebuia*, and *Smilax* (Fig. 6). *Spiniferites* (a dinoflagellate) is an indicator of warm waters (Price *et al*., 2013) and its presence is consistent with a warmer climate (Fig. 7). The change into current conditions probably started during this time, with a strengthening of seasonality and a slight reduction of torrential rainfalls, facilitating the establishment of the Cerrado biome (i.e. dry season with ~4-5 months). Semi-arid conditions prevailed in the northeast, while southern Brazil and western Amazonia returned to humid and very humid climates, respectively, typical of today (Aziz Ab'Sáber, 2003).

The last ~740 years exhibit very minor variations suggesting no significant changes in climate. However, all pollen taxa representative of the range of vegetation communities gradually decrease, except for the dry grassland (*Amarathus*, and in general the Amaranthaceae family; Fig. 6).

Discussion

Our findings demonstrate that the climate in central-eastern Brazil underwent several significant changes during the last ~35k cal a BP, mainly related to rainfall variability, but also, to some extent, to temperature variations as inferred from vegetation dynamics. Consequently, these changes are also reflected in different landscape conditions. Five main phases could be established: (C I) between ~35.0 to ~29.6k cal a BP – the climate was dry and warm with cooling events and some landscape instability; (C II) ~29.6 to ~16.9k cal a BP – wet and (C III) ~16.9 to ~6.1k cal a BP – very wet, both very cold and with reduced landscape instability; (C IV) ~6.1 to ~3.1k cal a BP – very dry and warm with increasing catchment instability; and (C V) < ~3.1k cal a BP – from dry and warm to sub-humid climate (Fig. 8).

The low humidity during MIS 3 suggested by our data coincides with the expansion of sea-ice and very low temperatures in the northern hemisphere (Heinrich, 1988; Dansgaard *et al*., 1993; Grootes and Stuiver,1997; Fig. 4B). These conditions may have resulted in the displacement of the ITCZ and, consequently, also the SACZ to a southward position (Fig. 8), leading to an increase in monsoon rainfall activity mainly in the south (Wang *et al*., 2004). The northern limit of the SACZ was probably located south of our study area, more than several hundred kilometers away from its present northern limit (Fig. 1). Millennial-scale rainfall variability is the dominant control during MIS 3, but increased rainfall is also possibly related to the strengthening of the SAMS resulting from high summer insolation in certain periods, and apparently in phase with $\delta^{13}C$ and austral summer insolation (ASI) (Fig. 4A1).

During the last precession cycle (the last ~17 ka) strong convective activity and upward motion resulted in enhanced condensational heating over the western Amazon Basin when ASI was high, which in turn intensified the upper-tropospheric Nordeste low and resulted in large-scale subsidence and humidity reduction over eastern equatorial South America (Cheng *et al*., 2013). According to these authors, this is the east-west dipole-like pattern of precipitation changes, also called the South American precipitation dipole (SAPD). It is also seen in our record from the

beginning of the late Pleistocene to the present, particularly after the ~16.9k cal a BP event, in alignment with the same trends in northeastern Brazil, including an antiphase with ASI (Fig. 8). This means that the increased precipitation occurred during weak monsoon seasons when ASI was low since ~16.9k cal a BP when precipitation was related to insolation. However, it is not yet clear if orbital-scale variability is the dominant control on precipitation after H1 and YD events. In the northern hemisphere, abrupt temperature increases may have caused changes in the Atlantic meridional overturning circulation and SACZ location, with the latter possibly shifted northward providing more humidity to central-eastern Brazil.

The SAPD can be probably applied to the LGM with some consistency as seen in records from other regions (Cheng *et al*., 2013). However, the relation is in phase for our study area, or the effect of precession was likely significantly reduced at millennial-scale, in periods when temperatures in the northern hemisphere began to slightly increase and SACZ was starting to shift northward.

Our study shows climate forcing operating at different timescales. During the last ~16.9k cal a BP, the orbital-scale variability is the dominant control, or both millennial and orbital-scale act together suggesting a common forcing. This mechanism is particularly important for tropical precipitation, as during these times changes in the eccentricity of the Earth's orbit promoted the modification to precessional forcing – hereafter defined as the ''precessionally forced'' or ''orbitally forced'' changes in insolation –, with predominant periods at 19 ka and 23 ka (Liu and Battisti, 2015). However, the millennial-scale is expressed through all the ~35k cal a BP record , to a greater or lesser extent, which allows to track the swings of the SACZ (Fig. 8): SACZ I - it shifted to a southward position in MIS 3, very near to Botuverá cave in Santa Catarina state (number 3, Fig. 1); SACZ II - a northward shift during the LGM, with a northern limit probably located near or within the location of the Pinheiro mire in Minas Gerais state (number 1, Fig. 1); SACZ III – a shift further northward, remaining stable for all this time over the Pinheiro mire from LP to MH (until

~6.1k cal a BP), with all the band within the central-eastern Brazil; and SACZ IV – a return to a southward position. Today the SACZ is located between the central-eastern and southeastern regions of Brazil (20°–40°S and 50°–20°W) (Barreiro *et al*., 2002).

The precipitation pattern for central-eastern Brazil reconstructed in this study is out of phase with western Amazonia and, apparently, with southern Brazil (Cheng *et al*., 2013). For southern Brazil, some periods of increased humidity appear to coincide with those found in our record. Concerning the northeast, our record is in phase from ~35 to ~26k cal a BP (considering the absence of speleothem deposition), out of phase from ~26 to ~16.9k cal a BP, and in phase again after ~16.9k cal a BP.

The current sub-humid climatic conditions and predominant Cerrado biome vegetation seem to be relatively recent, probably established after ~3.1k cal a BP; although similar conditions may have been present in MIS 3, mainly between ~35.0 to ~29.6k cal a BP. Pollen records from Lagoa de Serra Negra (De Oliveira, 1992) and Lagoa Santa (Parizzi, 1993) also showed the expansion of the Cerrado elements during the late Holocene, suggesting favourable conditions for this biome. Similarly, Werneck *et al*. (2012) also verified the expansion of the Cerrado in this period by investigating the historical distribution of the Cerrado across Quaternary climatic fluctuations. Today, semi-deciduous (seasonal) and mountain (cold) forests, so-called Capões, are relicts of wetter climates, indicating long-term climate variability during the Quaternary, since they were much more developed in the past, especially between ~29.6 and ~6.1k cal a BP. During the Mid-Holocene, more humid climate was also prevalent in other current areas of Cerrado, as in Águas Emendadas (Barberi *et al*., 2000) and Crominia palm swamp (Ferraz-Vicentini and Salgado-Labouriau, 1996; Barberi *et al*., 2000). This can be considered as key information on the origin of tropical plant biodiversity.

463 Pinheiro mire certainly contains a sensitive record of climate variability when compared to
464 other records (mires, speleothems, lake, and marine sediments) from previous studies (Fritz *et al*.,
465 2007; Stríkis *et al*., 2015), which is mainly due to its position being influenced by the constant
466 fluctuation and displacement of the SACZ.

467 Conclusions

468 The multi-proxy investigation of the Pinheiro mire (PI core) enhances our knowledge about
469 the relationship between past climate and vegetation change in central-eastern Brazil. We show
470 environmental and climate changes from late Pleistocene at millennial and orbital timescales and
471 the displacements of the SACZ. Our work contributes to one of the current most controversial
472 debates about the nature of climate during the Last Glacial Maximum (LGM) and mid-Holocene
473 (MH) (between ~29.6 and ~6.1k cal a BP), which were not dry for the studied region. On the
474 contrary, we suggest that these periods were the most humid of the last ~35k cal a BP.

475 The current vegetation on the Pinheiro mire has taxa that were part of the vegetation in past
476 periods. These taxa attest for past climatic conditions, such as the presence of trees and shrubs with
477 thick bark and tortuous trunks typical of savanna in more drier periods, as seen almost constantly
478 during the Marine Isotope Stage 3, and even the modern forest islands – the Capões –, with typical
479 taxa that resemble the forest of very wet climates occurred since the LGM up until the mid-
480 Holocene. However, it is important to note that the taxa were rearranged during the Quaternary and
481 the communities readjusted by undergoing a certain modification, mainly due to changes in climate.

482 Thus, the Pinheiro mire proved to be an insightful archive of past changes, showing its high
483 scientific importance - a good reason for its preservation.

484 Figure legends

485 **Figure 1.** Long-term mean (A.D. 1979-2000) precipitation (mm) for December-February (DJF)
486 from the Climate Prediction Center Merged Analysis of Precipitation. Numbers in the map indicate
487 the study site and other climate records from South America: 1 - Pinheiro mire in Minas Gerais
488 state, central-eastern Brazil; 2 - Rio Grande do Norte caves in Rio Grande do Norte state,
489 northeastern Brazil (Cruz *et al*., 2009); 3 - Botuverá cave in Santa Catarina state, southern Brazil
490 (Cruz *et al*., 2005); and 4 - western Amazonia caves, northern Peru (Cheng *et al*., 2013). ITCZ -
491 Intertropical Convergence Zone; SACZ - South Atlantic Convergence Zone; LLJ - low-level jet.

492 **Figure 2.** (A) Satellite image of the Pinheiro mire location (drains from SW to NE situated between
493 1270 and 1230 m a.s.l.) obtained from Google Earth. (B) Photo of the sampling site - Pinheiro mire
494 (valley mire and minerogenic under wet grassland). (C) Stratigraphy of the PI core. Oi and Oa are
495 fibric and sapric peat layers, respectively; C are sediment layers.

496 **Figure 3.** Age-depth model of the PI core fitted with Bacon (Blaauw and Christen, 2011) using the
497 dating for the peat samples of the upper meter of the core (blue) and Southern Hemisphere
498 calibration curve (SHCal13.14C).

499 **Figure 4.** Comparison between South America records over the past 35 ka BP. (A1) $\delta^{13}C$; (A2)
500 $\delta^{15}N$; (A3) Cp2; and (A4) Br/C ratio of the Pinheiro record, central-eastern Brazil. (B) Greenland
501 ice (GISP2) $\delta^{18}O$ record (Grootes and Stuiver, 1997). (C) Rio Grande do Norte speleothem $\delta^{18}O$
502 record, northeastern Brazil. (D) Botuverá speleothem $\delta^{18}O$ record, southern Brazil. (E) western
503 Amazonia speleothem $\delta^{18}O$ record, northern Peru. The red curves represent austral summer (DJF)
504 insolation (ASI) (Berger, 1978). Gray bars show periods of increased humidity in central-eastern
505 Brazil. MIS 3 = Marine Isotope Stage 3; LGM = Last Glacial Maximum; LP = late Pleistocene; EH
506 = early Holocene; MH = middle Holocene; and LH = late Holocene.

507 **Figure 5.** Distribution of the main taxa by type of vegetation or environment of the PI core. The
508 silhouettes show the percentage curves, while shades show the 4x exaggeration curves. CONISS

cluster analysis together with the Palynological Zones (separated by dashed lines) are plotted. Values are expressed as percentages of the total land pollen sum (TLP).

Figure 6. Synthetic regional (total land pollen sum) palynological diagram of the PI core. The silhouettes show the percentage curves of the taxa, while shades show the 4x exaggeration curves. CONISS cluster analysis together with the Regional Palynological Zones (RPZ; separated by dashed lines) are plotted. Values are expressed as percentages of the total land pollen sum (TLP). Green: trees; blue: trees/shrubs; yellow: herbs; and purple: lianas.

Figure 7. Synthetic local (hydro-hygrophytes and NPP) palynological diagram of the PI core. The silhouettes show the percentage curves of the taxa, while shades show the 4x exaggeration curves. CONISS cluster analysis together with the Local Palynological Zones (LPZ) are plotted. Values are expressed as percentages of the total land pollen sum (TLP). Blue: hydro-hygrophytes; green: pteridophytes; purple: algae; red: fungi; and yellow: dinoflagellates.

Figure 8. Chronology of Pleistocene environmental changes recorded in the PI core. MIS 3 = Marine Isotope Stage 3; LGM = Last Glacial Maximum; LP = late Pleistocene; EH = early Holocene; MH = middle Holocene; and LH = late Holocene. ASI = austral summer insolation. SACZ I to SACZ IV: swings of the South Atlantic convergence zone (SACZ). RPZ and LPZ are palinozones of regional and local vegetation, respectively. C I to C V: phases of environmental change. Orange: dry; yellow: very dry; light blue: wet; dark blue: very wet; and purple: sub-humid climatic.

Supporting Information

Additional supporting information may be found online in the Supporting Information section at the end of the article.

Figure S1. Age-depth model of the PI core fitted with Bacon (Blaauw & Christen, 2011) using the dating for the peat samples of the upper meter of the core (blue) and Northern Hemisphere calibration curve (IntCal13).

Figure S2. Records of factor scores of the three components of PCA (Cp1, Cp2, and Cp3) for the geochemical composition of the PI core.

Figure S3. Factor loadings for the three components and fractionation of communalities of the variables used in the PCA of geochemical properties of the PI core. The communality of each variable (i.e. the proportion of its variance explained by each component) corresponds to the total length of the bar, and the sections of the bars represent the proportion of variance in each component. The variables are ordered by the component with the largest share of variance. [1]Eigenv: eigenvalues; [2]Var (%): percentage of explained variance; 3Var_ac: cumulative explained variance.

Figure S4. Contents (in %) of ash, fiber, C and N; BD (bulk density; in Mg m^{-3}); and $\delta^{13}C$ and $\delta^{15}N$ (in **‰)** of the PI core.

Figure S5. Concentrations (in g kg^{-1}) of Si, Al, Fe, Ti, K, Ca, S, and P of the PI core.

Figure S6. Concentrations (in µg g^{-1}) of Ga, Rb, Sr, Zr, Y, and Nb of the PI core.

Figure S7. Concentrations (in µg g^{-1}) of Mn, Th, Cr, Pb, Cl, and Br of the PI core.

Figure S8. Regional (total land pollen sum) palynological diagram of the PI record with taxa not included in the Figure 6. The silhouettes show the percentage curves of the taxa, while shades show 14x (Figure S8A) and 12x exaggeration curves (Figure S8B). CONISS cluster analysis together with the Regional Palynological Zones (RPZ; separated by dashed lines) are plotted. Values are

551 expressed as percentages of the total land pollen sum (TLP). In Figure S8A: Green: trees; blue:
552 trees/shrubs; and purple: shrubs. In Figure S8B: Yellow: herbs; light blue: lianas; and red: diverses.

553 **Figure S9.** Local (hydro-hygrophytes and NPP) palynological diagram of the PI record with taxa
554 not included in the Figure 7. The silhouettes show the percentage curves of the taxa, while shades
555 show 10x exaggeration curves. CONISS cluster analysis together with the Local Palynological
556 Zones (LPZ; separated by dashed lines) are plotted. Values are expressed as percentages of the total
557 land pollen sum (TLP). In Figure S9A: Blue: hydro-hygrophytes; light blue: bryophyte; and green:
558 pteridophytes. In Figure S9B: Purple: algae; red: fungi; and yellow: dinoflagellates.

559 **Table S1.** Results of ^{14}C dating of the PI core, showing conventional age in a BP and calibrated
560 ages (2σ) in cal a BP.

561 **Table S2.** The maximum number of total land pollen (TLP) and hydro-hygrophytes and non-pollen
562 palynomorphs (NPP) of the PI core.

563 **Table S3.** Pollen and other non-pollen palynomorphs (NPP) observed in PI core, their habit,
564 coverage, and phytophysiognomy belonging or probable environmental indicator.

565 *Acknowledgments.* This work was supported by Fundação de Amparo à Pesquisa do Estado de São
566 Paulo (FAPESP)/Brazil (grant to I.H.T - regular doctoral scholarship FAPESP 2010/51637-0 and
567 research internships abroad BEPE/FAPESP 2012/00676-1), Conselho Nacional de
568 Desenvolvimento Científico e Tecnológico (CNPq)/Brazil (Universal 14/2011 – 482815/2001-6),
569 Ministério de Economia y Competitividad (CGL2010-20662) and Xunta de Galícia
570 (10PXIB200182PR, ED431D2917/08 and ED431B2018/20). We are grateful to Noemí Silva
571 Sánchez and Luis Rodriguez Lado (Univesidad de Santiago de Compostela), and Fabrício da Silva
572 Terra (Universidade Federal dos Vales do Jequitinhonha e Mucuri) for their collaboration and
573 assistance during different stages of the research.

References

Alvares CA, Stape JL, Sentelhas PC *et al.* 2013. Köppen's climate classification map for Brazil. *Meteorologische Zeitschrift* **22**: 711 - 728, https://doi.org/10.1127/0941-2948/2013/0507

Arruda DM, Schaefer CEGR, Fonseca RS *et al*. 2017. Vegetation cover of Brazil in the last 21 ka: New insights into the Amazonian refugia and Pleistocenic arc hypotheses. *Global Ecology and Biogeography* **27**: 47-56, https://doi.org/10.1111/geb.12646

Aziz Ab'Sáber. 2003. Os domínios de Natureza no Brasil – Potencialidades Paisagísticas. Atêlie Editorial: São Paulo.

Barberi M, Salgado-Labouriau ML, Suguio K. 2000. Paleovegetation and paleoclimate of "Vereda de Águas Emendadas", central Brazil. *Journal of South American Earth Sciences* **13**: 241-254, https://doi.org/10.1016/S0895-9811(00)00022-5

Barreiro M, Chang P, Saravanan R. 2002. Variability of the South Atlantic Convergence Zone Simulated by an Atmospheric General Circulation Model. *Journal of Climate* **15**: 745-763, https://doi.org/10.1175/1520-0442(2002)015<0745:VOTSAC>2.0.CO;2

Berger, AL. 1978. Long-term variations of caloric insolation resulting from the Earth's orbital elements. *Quaternary Research* **9**: 139–167, https://doi.org/10.1016/0033-5894(78)90064-9

Biester H, Martínez Cortizas A, Keppler F. 2006. Occurrence and fate of halogens in mires. In *Peatlands: Evolution and Records of Environmental and Climate Changes,* Martini IP, Martínez Cortizas A, Chesworth W (eds). Elsevier BV: Amsterdam; 449–464.

Blaauw M, Christen JA. 2011. Flexible paleoclimate age-depth models using an autoregressive gamma process. *Bayesian Analysis* **6**: 457–474, https://doi.org/10.1214/11-BA618

Boutton TW. 1991. Stable Carbon Isotope Ratios of Natural Materials: 2. Atmospheric, Terrestrial, Marine, and Freshwater Environments. In *Carbon isotopes techniques,* Coleman DC, Fry B (eds). Academic Press, Inc: San Diego; 173-185.

Bronk Ramsey C. 2008. Deposition models for chronological records. *Quaternary Science Reviews* **27**: 42-60, https://doi.org/10.1016/j.quascirev.2007.01.019

Bucher EH. 1982. Chaco and Caatinga — South American Arid Savannas, Woodlands and Thickets. In *Ecology of Tropical Savannas,* Huntley BJ, Walker BH (eds). Springer-Verlag: Berlin; 48–79.

Bueno ML, Pennington RT, Dexter KG *et al*. 2016. Effects of quaternary climatic fluctuations on the distribution of Neotropical savanna tree species. *Ecography* **40:** 403–414, https://doi.org/10.1111/ecog.01860

Cerling TE, Quade J, Wang Y *et al*. 1989. Carbon isotopes in soils and paleosols as ecology and paleoecology indicators. *Nature* **341**: 138-139, https://doi.org/10.1038/341138a0

Cheburkin AK, Shotyk W. 1996. An Energy-dispersive Miniprobe Multielement Analyzer (EMMA) for direct analysis of Pb and other trace elements in peats. *Fresenius Journal Analytical Chemistry* **354**: 688-691, https://doi.org/10.1007/s0021663540688

Cheng H, Sinha A, Cruz FW *et al*. 2013. Climate change patterns in Amazonia and biodiversity. *Nature Communications* **4**: 1411, https://doi.org/0.1038/ncomms2415

Colinvaux PA, De Oliveira PE, Moreno, JE *et al*. 1996. A long pollen record from lowland Amazonia: Forest and cooling in glacial times. *Science* **274**: 85–88, https://doi.org/10.1126/science.274.5284.85

Cruz FWJ., Burns SJ, Karmann I *et al*. 2005. Insolation driven changes in atmospheric circulation over the past 116,000 years in subtropical Brazil. *Nature* **434**: 63–66, https://doi.org/0.1038/nature03365

Cruz FW, Vuille M, Burns SJ *et al*. 2009. Orbitally driven east–west antiphasing of South American precipitation. *Nature Geoscience* **2**: 210–214, https://doi.org/10.1038/NGEO444.

Dansgaard W, Johnsen SJ, Clausen HB *et al*. 1993. Evidence for general instability of past climate from a 250-kyr ice-core record. *Nature* **364**: 218-220, https://doi.org/10.1038/364218a0

De Oliveira, PE. 1992. A palynological record of Late Quaternary vegetational and climatic change in southeastern Brazil. Doctoral thesis. *The Ohio State University*.

De Oliveira PE, Raczka M, McMichael CNH *et al*. 2019. Climate change and biogeographic connectivity across the Brazilian cerrado. *Journal of Biogeography 47*: 396-407, https://doi.org/10.1111/jbi.13732

Dommain R, Couwenberg J, Joosten H. 2011. Development and carbon sequestration of tropical peat domes in south-east Asia: links to post-glacial sea-level changes and Holocene climate variability. *Quaternary Science Reviews* **30**: 999–1010, https://doi.org/10.1016/j.quascirev.2011.01.018

Eriksson L, Johansson E, Kettaneh-Wold N *et al*. 1999. Introduction to multi- and megavariate data analysis using projection methods (PCA & PLS). Umetrics AB: Umea.
FAO. 2006. Guidelines for soil description. Management Service: Rome.
Ferraz-Vincentini KR, Salgado-Labouriau ML. 1996. Palynological analysis of a palm swamp in Central Brazil. *Journal of South American Earth Sciences* **9**: 207-219, https://doi.org/10.1016/0895-9811(96)00007-7
Fritz SC, Baker PA, Seltzer GO *et al*. 2007. Quaternary glaciation and hydrologic variation in the South American tropics as reconstructed from the Lake Titicaca drilling project. *Quaternary Research* **68**: 410-420, https://doi.org/10.1016/j.yqres.2007.07.008
Garreaud RD, Vuille M, Compagnucci R *et al*. 2009. Present-day South American climate. *Palaeogeography Palaeoclimatology Palaeoecology* **281**: 180–195, https://doi.org/10.1016/j.palaeo.2007.10.032
Goldblatt P. 1978. An analysis of the flora of Southern Africa: Its characteristics, relationships, and origins. *Annals of Missouri Botanical Garden* **65**: 369-436, https://doi.org/10.2307/2398858
Grimm EC. 1987. CONISS: a FORTRAN 77 program for stratigraphically constrained cluster analysis by the method of incremental sum of squares. *Computers & Geosciences* **13**: 13-35, https://doi.org/10.1016/0098-3004(87)90022-7
Grootes PM, Stuiver M. 1997. Oxygen 18/16 variability in Greenland snow and ice with 103 to 105-year time resolution. *Journal of Geophysical Research* **102**: 26455–26470, https://doi.org/10.1029/97JC00880
Haberle SG, Maslin MA. 1999. Late Quaternary vegetation and climate change in the Amazon Basin based on a 50,000 year pollen record from the Amazon Fan, ODP Site 932. *Quaternary Research* **51**: 27–38, https://doi.org/10.1006/qres.1998.2020
Haffer J. 1969. Speciation in Amazonian forest birds. *Science* **165**: 131–137. https://doi.org/10.1126/science.165.3889.131
Heinrich H. 1988. Origin and consequences of cyclic ice rafting in the Northeast Atlantic Ocean during the past 130,000 years. *Quaternary Research* **29**: 142-152, https://doi.org/10.1016/0033-5894(88)90057-9
Hogg AG, Hua Q, Blackwell PG *et al*. 2013. ShCal13 Southern Hemisphere calibration, 0-50,000 cal yr BP. *Radiocarbon* **55**: 1889–1903, https://doi.org/10.2458/azu_js_rc.55.16783
Horák I. 2009. Relações pedológicas, isotópicas e palinológicas na reconstrução paleoambiental da turfeira da Área de Proteção Especial (APE) Pau-de-Fruta, Serra do Espinhaço Meridional – MG. Master Dissertation. *Escola Superior de Agricultura Luiz de Queiroz - Universidade de São Paulo*.
Horák-Terra I. 2014. Late Pleistocene-Holocene environmental change in Serra do Espinhaço Meridional (Minas Gerais State, Brazil) reconstructed using a multi-proxy characterization of peat cores from mountain tropical mires. Doctoral thesis. *Escola Superior de Agricultura Luiz de Queiroz - Universidade de São Paulo*.
Horák-Terra I, Martínez Cortizas A, de Camargo PB *et al*. 2014. Characterization of properties and main processes related to the genesis and evolution of tropical mountain mires from Serra do Espinhaço Meridional, Minas Gerais, Brazil. *Geoderma* **232–234**: 183–197, https://doi.org/10.1016/j.geoderma.2014.05.008
Horák-Terra I, Martínez Cortizas A, Luz CFP *et al*. 2015. Holocene climate change in central-eastern Brazil reconstructed using pollen and geochemical records of Pau de Fruta mire (Serra do Espinhaço Meridional, Minas Gerais). *Palaeogeography Palaeoclimatology Palaeoecology* **437:** 117-131, https://doi.org/10.1016/j.palaeo.2015.07.027
Juggins S. 2019. Rioja: analysis of Quaternary science data, R package version 0.9-21.cran.r-project.org/package=rioja.
Kanner LC, Burns SJ, Cheng H *et al*. 2012. High latitude forcing of the South American Summer Monsoon during the Last Glacial. *Science* **335**: 570–573, https://doi.org/10.1126/science.1213397
Keith SA, Newton AC, Herbert RJH *et al*. 2009. Non-analogous community formation in response to climate change. *Journal for Nature Conservation* **17**: 228—235, https://doi.org/10.1016/j.jnc.2009.04.003
Klink CA, Machado RB. 2005. Conservation of the Brazilian Cerrado. *Conservation Biology* **19**: 707–713, https://doi.org/10.1111/j.1523-1739.2005.00702.x
Knauer LG. 2007. O Supergrupo Espinhaço em Minas Gerais: considerações sobre sua estratigrafia e seu arranjo estrutural. *Geonomos* **15**: 81−90.
Lalor G. 1995. A geochemical atlas of Jamaica. Canoe Press University of the West Indies: Jamaica.
Ledru M-P, Salgado-Labouriau ML, Lorscheitter ML. 1998. Vegetation dynamics in southern and central Brazil during the last 10,000 yr B.P. *Review of Palaeobotany and Palynology* **99**: 131–142, https://doi.org/10.1016/S0034-6667(97)00049-3

Ledru M-P, Mourguiart P, Riccomini C. 2009. Related changes in biodiversity, insolation and climate in the Atlantic rainforest since the last interglacial. *Palaeogeography Palaeoclimatology Palaeoecology* **271**: 140-152, https://doi.org/10.1016/j.palaeo.2008.10.008

Leite YLR, Costa LP, Loss AC. 2016. Neotropical forest expansion during the last glacial period challenges refuge hypothesis. *Proceedings of the National Academy of Sciences of the United States of America* **113**: 1008–1013, https://doi.org/10.1073/pnas.1513062113

Liu X, Battisti DS. 2015. The Influence of Orbital Forcing of Tropical Insolation on the Climate and Isotopic Composition of Precipitation in South America. *Journal of Climate* **28**: 4841-4862, https://doi.org/10.1175/JCLI-D-14-00639.1

Luz CFP da, Horák-Terra I, Silva AC *et al*. 2017. Pollen record of a tropical peatland (Pau de Fruta) from the Serra do Espinhaço Meridional, Diamantina, State of Minas Gerais – Angiosperms Eudicotyledons. *Revista Brasileira de Paleontologia* **20(1)**: 3-22, http://dx.doi.org/10.4072/rbp.2017.1.01

Marchant R, Almeida L, Behling H *et al*. 2002. Distribution and ecology of parent taxa of pollen lodged within the Latin America Pollen Database. *Review of Palaeobotany and Palynology* **121**: 1-75, https://doi.org/10.1016/S0034-6667(02)00082-9

Martin L, Flexor JM, Suguio K. 1995. Vibrotestemunhador leve: construção, utilização e possibilidades. *Revista do Instituto Geológico* **16**: 59-66, http://doi.org/10.5935/0100-929X.19950004

Martinelli LA, Ometto JPHB, Ferraz ES *et al*. 2009. Desvendando questões ambientais com isótopos estáveis. Oficina de textos: Brazil.

Mendonça RC, Felfili JM, Walter BMT *et al*. 1998. Flora vascular do cerrado. In *Cerrado: ambiente e flora,* Sano SM, Almeida SP (eds). Embrapa: Brazil; 289-556.

Muller J, Kylander M, Wüst RAJ *et al*. 2008. Possible evidence for wet Heinrich phases in tropical NE Australia: the Lynch's Crater deposit. *Quaternary Science Reviews* **27**: 468–475, https://doi.org/10.1016/j.quascirev.2007.11.006

O'Leary MH. 1988. Carbon isotopes in photosynthesis. *BioScience* **38**: 328-336, https://doi.org/10.2307/1310735

Parizzi MG. 1993. A gênese e a dinâmica da Lagoa Santa com base em estudos palinológicos, geomorfológicos e geológicos de sua bacia. Master Dissertation. *Universidade Federal de Minas Gerais*.

Pennington RT, Lewis GP, Ratter JA. 2006. An overview of the plant diversity, biogeography and conservation of neotropical savannas and seasonally dry forests. In *Neotropical savannas and dry forests*: *Plant diversity, biogeography and conservation*, Pennington RT, Lewis GP, Ratter, JA (eds). CRC Press: Boca Raton; 1-29.

Pérez-Rodríguez M, Horák-Terra I, Rodríguez-Lado L *et al*. 2015. Long-Term (~57 ka) Controls on Mercury Accumulation in the Souther Hemisphere Reconstructed Using a Peat Record from Pinheiro Mire (Minas Gerais, Brazil). *Environmental Science & Technology* **49**: 1356-1364, https://doi.org/10.1021/es504826d

Pérez-Rodríguez M, Horák-Terra I, Rodríguez-Lado L *et al.* 2016. Modelling mercury accumulation in minerogenic peat combining FTIR-ATR spectroscopy and partial least squares (PLS). *Spectrochimica Acta Part A: Molecular and Biomolecular Spectroscopy* **168**: 65-72, https://doi.org/10.1016/j.saa.2016.05.052

Pinaya J, Cruz F, Ceccantini G *et al*. 2019. Brazilian montane rainforest expansion induced by Heinrich Stadial 1 event. *Scientific Reports* **9**: 1-14, https://doi.org/10.1038/s41598-019-53036-1

Prado DE, Gibbs PE. 1993. Patterns of species distributions in the dry seasonal forests of South America. *Annals of the Missouri Botanical Garden* **80**: 902–927, https://doi.org/10.2307/2399937

Price AM, Mertens KN, Pospelova V *et al*. 2013. Late Quaternary climatic and oceanographic changes in the Northeast Pacific as recorded by dinoflagellate cysts from Guaymas Basin, Gulf of California (Mexico). *Paleoceonagraphy and Paleoclimatology* **28**: 1-13, https://doi.org/10.1002/palo.20019

Reimann C, Filzmoser P, Garrett R *et al*. 2008. Statistical data analysis explained: Applied environmental statistics with R. John Wiley & Sons Ltd: Chichester.

Rizzini CT. 1979. Tratado de Fitogeografia do Brasil. HUCITEC, EDUSP: Brazil.

Rodríguez-Zorro PA, Ledru M-P, Bard E *et al.* 2020 Shut down of the South American summer monsoon during the penultimate glacial. *Scientific Reports* **10**: 6275, https://doi.org/10.1038/s41598-020-62888-x

Roubik DW, Moreno PJE. 1991. Pollen and spores of Barro Colorado Island. New York. Missouri Botanical Garden: Saint Louis.

Salgado-Labouriau, ML. 2007. Critérios e técnicas para o Quaternário. Blucher: São Paulo.

Schellekens J, Horák-Terra I, Buurman P *et al*. 2014. Holocene vegetation and fire dynamics in central-eastern Brazil: Molecular records from the Pau de Fruta peatland. *Organic Geochemistry* **77**: 32–42, https://doi.org/10.1016/j.orggeochem.2014.08.011

Schoeneberger PJ, Wysocki DA, Benham EC *et al*. 1998. Field book for describing and sampling soils. National Soil Survey Center: Lincoln.

Simon MF, Grether R, de Queiroz LP. 2009. Recent assembly of the Cerrado, a neotropical plant diversity hotspot, by in situ evolution of adaptations to fire. *Proceedings of the National Academy of Sciences of the United States of America* **106**: 20359-20364, https://doi.org/10.1073/pnas.0903410106

Soil Survey Staff. 2010. Keys to Soil Taxonomy. Natural Resources Conservation Service: Washington.

Stríkis NM, Cruz FW, Cheng H *et al*. 2011. Abrupt variations in South American monsoon rainfall during the Holocene based on a speleothem record from central–eastern Brazil. *Geology* **39**: 1075–1078, https://doi.org/10.1130/G32098.1

Stríkis NM, Chiessi CM, Cruz FW *et al*. 2015. Timing and structure of Mega-SACZ events during Heinrich Stadial. *Geophysical Research Letters* **42**: 5477-5484, https://doi.org/10.1002/2015GL064048

Swindles GT, Kelly TJ, Roucoux KH *et al*. 2018. Response of testate amoebae to a late Holocene ecosystem shift in an Amazonian peatland. *European Journal of Protistology* **64**: 13–19, https://doi.org/10.1016/j.ejop.2018.03.002

Tryon RM, Tryon AF. 1982. Ferns and allied plants with special reference to Tropical America. Springer-Verlag: New York.

van Geel B. 1978. A palaeoecological study of holocene peat bog sections in Germany and The Netherlands, based on the analysis of pollen, spores and macro- and microscopic remains of fungi, algae, cormophytes and animals. *Review of Palaeobotany and Palynology* **25**: 1-120, https://doi.org/10.1016/0034-6667(78)90040-4

Vera C, Higgins W, Amador J *et al*. 2006. Toward a unified view of the American monsoon systems. *Journal of Climate* **19**: 4977–5000, https://doi.org/10.1175/JCLI3896.1

Wang X, Auler AS, Lawrence Edwards R *et al*. 2004. Wet periods in northeastern Brazil over the past 210 kyr linked to distant climate anomalies. *Nature* **432**: 740–743, https://doi.org/10.1038/nature03067

Wang X, Auler AS, Lawrence Edwards R *et al*. 2006. Interhemispheric anti-phasing of rainfall during the last glacial period. *Quaternary Science Reviews* **25**: 3391–3403, https://doi.org/10.1016/j.quascirev.2006.02.009

Weiss D, Shotyk W, Cheburkin AK *et al*. 1998. Determination of Pb in the ash fraction of plants and peats using the Energy-dispersive Miniprobe Multielement Analyser (EMMA). *Analyst* **123**: 2097-2102, ttps://doi.org/10.1039/a805741i

Weiss D, Shotyk W, Rieley J *et al*. 2002. The geochemistry of major and selected trace elements in a forested peat bog, Kalimantan, SE Asia, and its implications for past atmospheric dust deposition. *Geochimica et Cosmochimica Acta* **66**: 2307-2323, https://doi.org/10.1016/S0016-7037(02)00834-7

Werneck FP, Costa GC, Colli GR *et al*. 2011. Revisiting the historical distribution of Seasonally Dry Tropical Forests: New insights based on palaeodistribution modelling and palynological evidence. *Global Ecology and Biogeography* **20**: 272–288, https://doi.org/10.1111/j.1466-8238.2010.00596.x

Werneck FP, Nogueira C, Colli GR *et al*. 2012. Climatic stability in the Brazilian Cerrado: implications for biogeographical connections of South American savannas, species richness and conservation in a biodiversity hotspot. *Journal of Biogeography* **39**: 1695–1706, https://doi.org/10.1111/j.1365-2699.2012.02715.x

Williams JW, Jackson ST. 2007. Novel climates, No-analog communities, and ecological surprises: Past and future. *Frontiers in Ecology and the Environment* **5**: 475–482, https://doi.org/10.1890/070037

Ybert JP, Salgado-Labouriau ML, Barth OM *et al*. 1992. Sugestões para padronização da metodologia empregada em estudos palinológicos do Quaternário. *Boletim do Instituto Geológico da USP* **13**: 47-49, http://dx.doi.org/10.5935/0100-929X.19920009

778
779
780
781
782
783
784
785
786
787
788
789
790
791
792
793
794
795
796
797
798
799
800
801
802
803

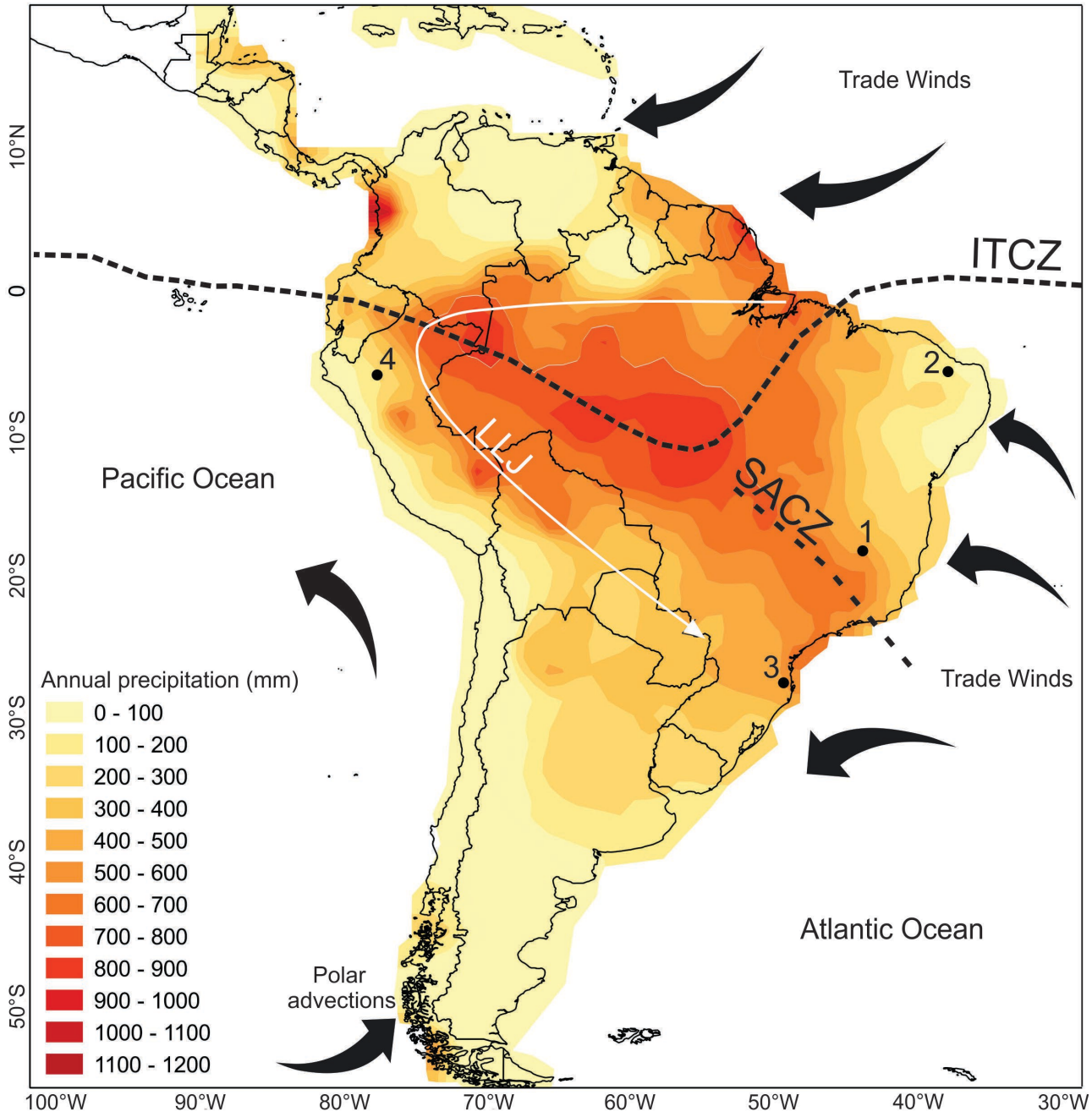
Trade Winds
ITCZ
4
2
LLJ
SACZ
1
Pacific Ocean
3
Trade Winds
Annual precipitation (mm)
0 - 100
100 - 200
200 - 300
300 - 400
400 - 500
500 - 600
600 - 700
700 - 800
800 - 900
900 - 1000
1000 - 1100
1100 - 1200
Atlantic Ocean
Polar
advections
10°N
0
10°S
20°S
30°S
40°S
50°S
100°W
90°W
80°W
70°W
60°W
50°W
40°W
30°W

Figure 1.

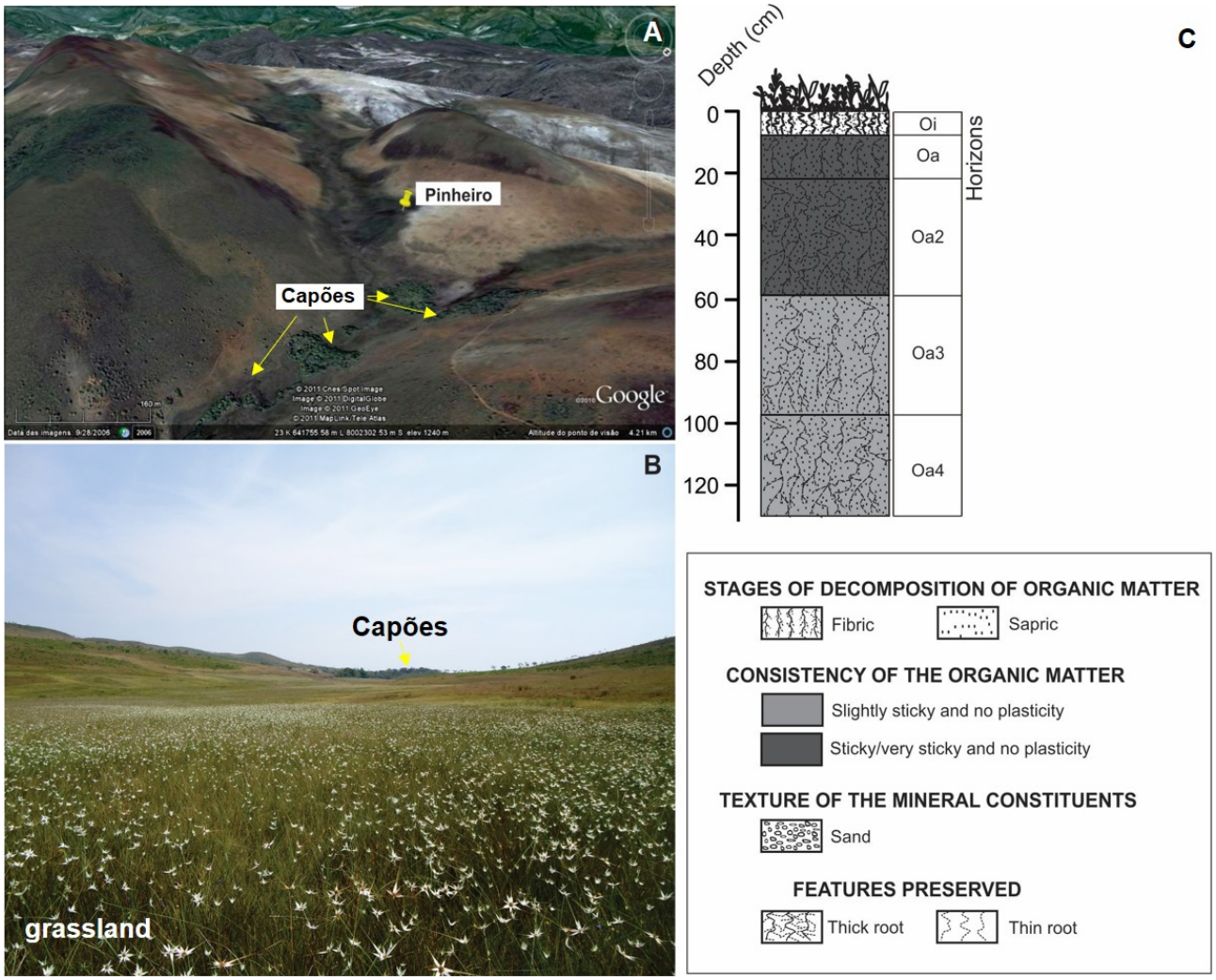
A
Pinheiro
Capões
B
Capões
grassland
C
Depth (cm)
0
20
40
60
80
100
120
Oi
Oa
Oa2
Oa3
Oa4
Horizons
STAGES OF DECOMPOSITION OF ORGANIC MATTER
Fibric
Sapric
CONSISTENCY OF THE ORGANIC MATTER
Slightly sticky and no plasticity
Sticky/very sticky and no plasticity
TEXTURE OF THE MINERAL CONSTITUENTS
Sand
FEATURES PRESERVED
Thick root
Thin root

Figure 2.

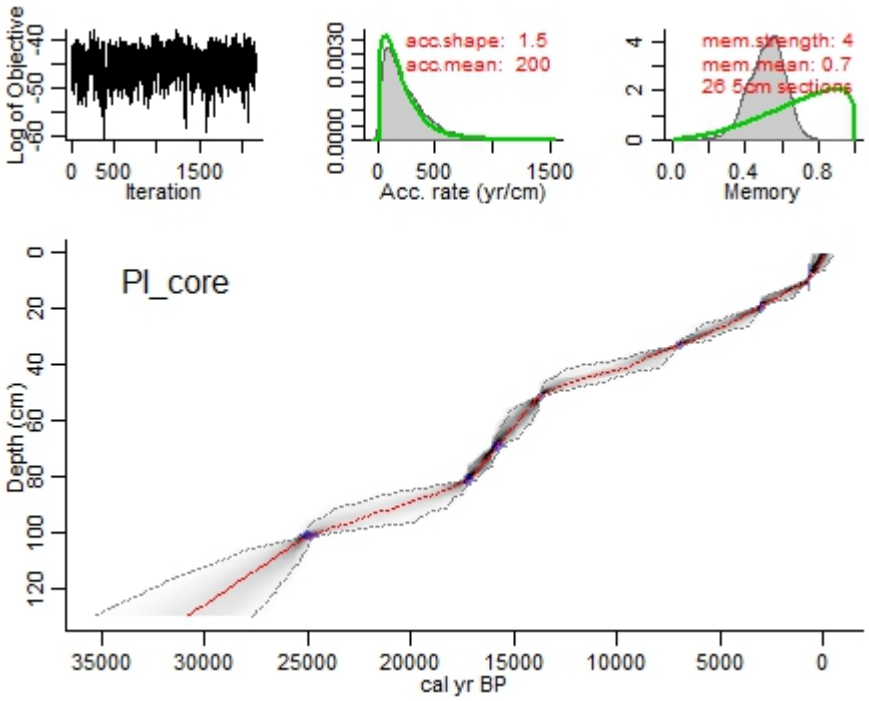
Log of Objective
-40
-50
-60
0 500 1500
Iteration
0.0030
0.0000
acc.shape: 1.5
acc.mean: 200
0 500 1500
Acc. rate (yr/cm)
4
2
0
mem.strength: 4
mem.mean: 0.7
26 5cm sections
0.0 0.4 0.8
Memory
Pl_core
Depth (cm)
0
20
40
60
80
100
120
35000 30000 25000 20000 15000 10000 5000 0
cal yr BP

Figure 3.

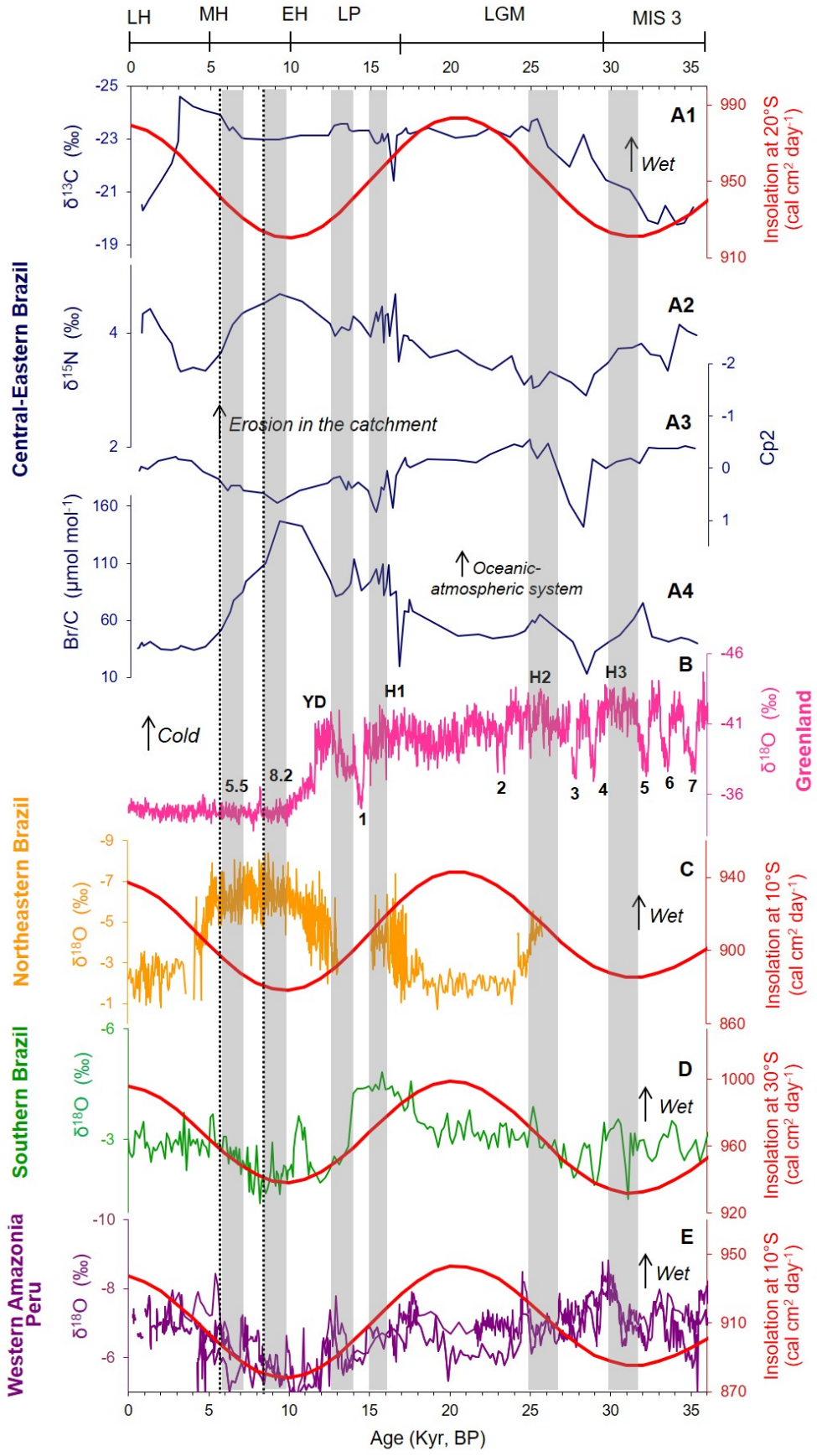
LH
MH
EH
LP
LGM
MIS 3
Central-Eastern Brazil
A1
A2
A3
A4
Wet
Erosion in the catchment
Oceanic-atmospheric system
Cold
δ13C (‰)
δ15N (‰)
Br/C (µmol mol-1)
Cp2
Insolation at 20°S (cal cm2 day-1)
B
YD
H1
H2
H3
5.5
8.2
1
2
3
4
5
6
7
δ18O (‰)
Greenland
Northeastern Brazil
C
Insolation at 10°S (cal cm2 day-1)
Southern Brazil
D
Insolation at 30°S (cal cm2 day-1)
Western Amazonia Peru
E
Age (Kyr, BP)

Figure 4.

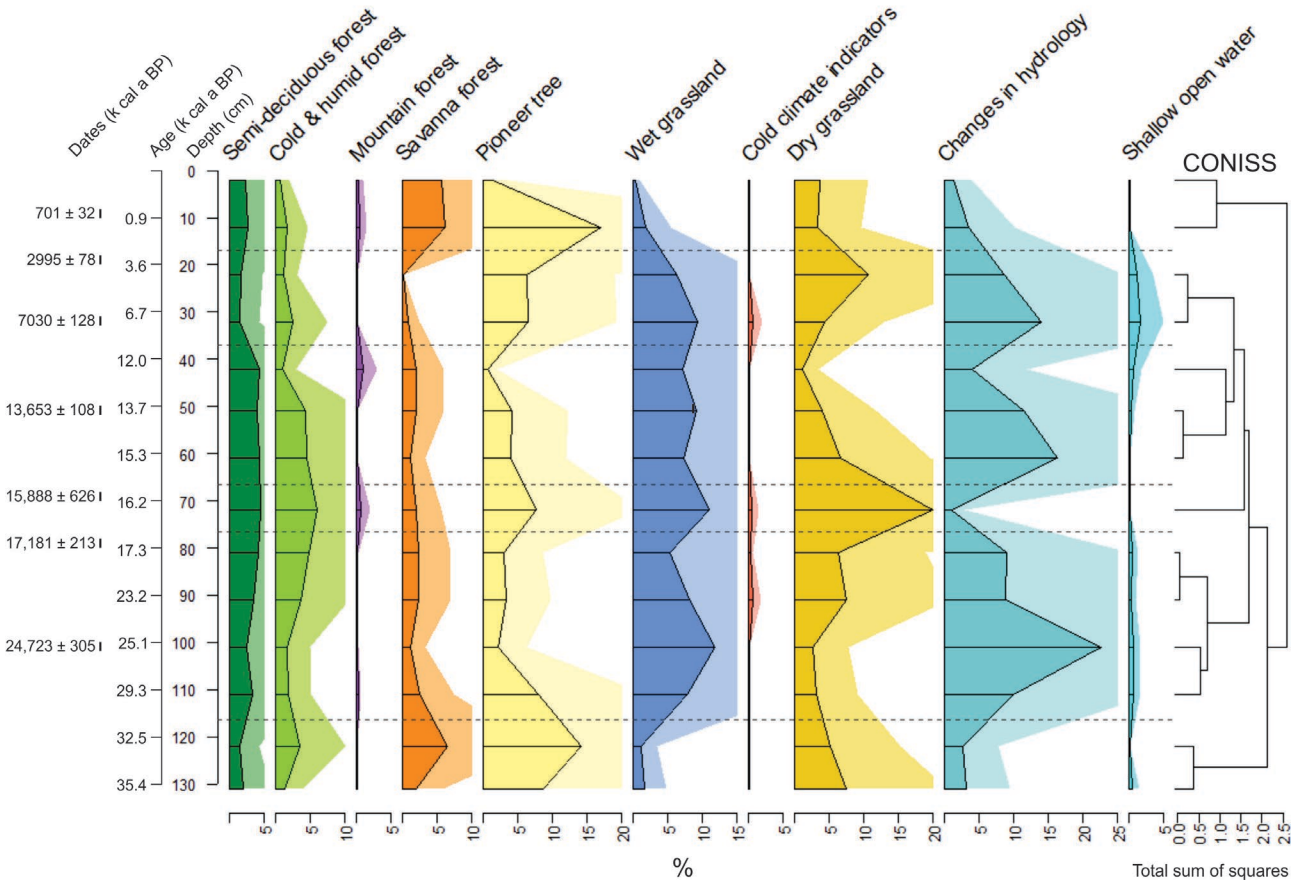
Dates (k cal a BP)
Age (k cal a BP)
Depth (cm)
Semi-deciduous forest
Cold & humid forest
Mountain forest
Savanna forest
Pioneer tree
Wet grassland
Cold climate indicators
Dry grassland
Changes in hydrology
Shallow open water
CONISS
701 ± 32
2995 ± 78
7030 ± 128
13,653 ± 108
15,888 ± 626
17,181 ± 213
24,723 ± 305
%
Total sum of squares

Figure 5.

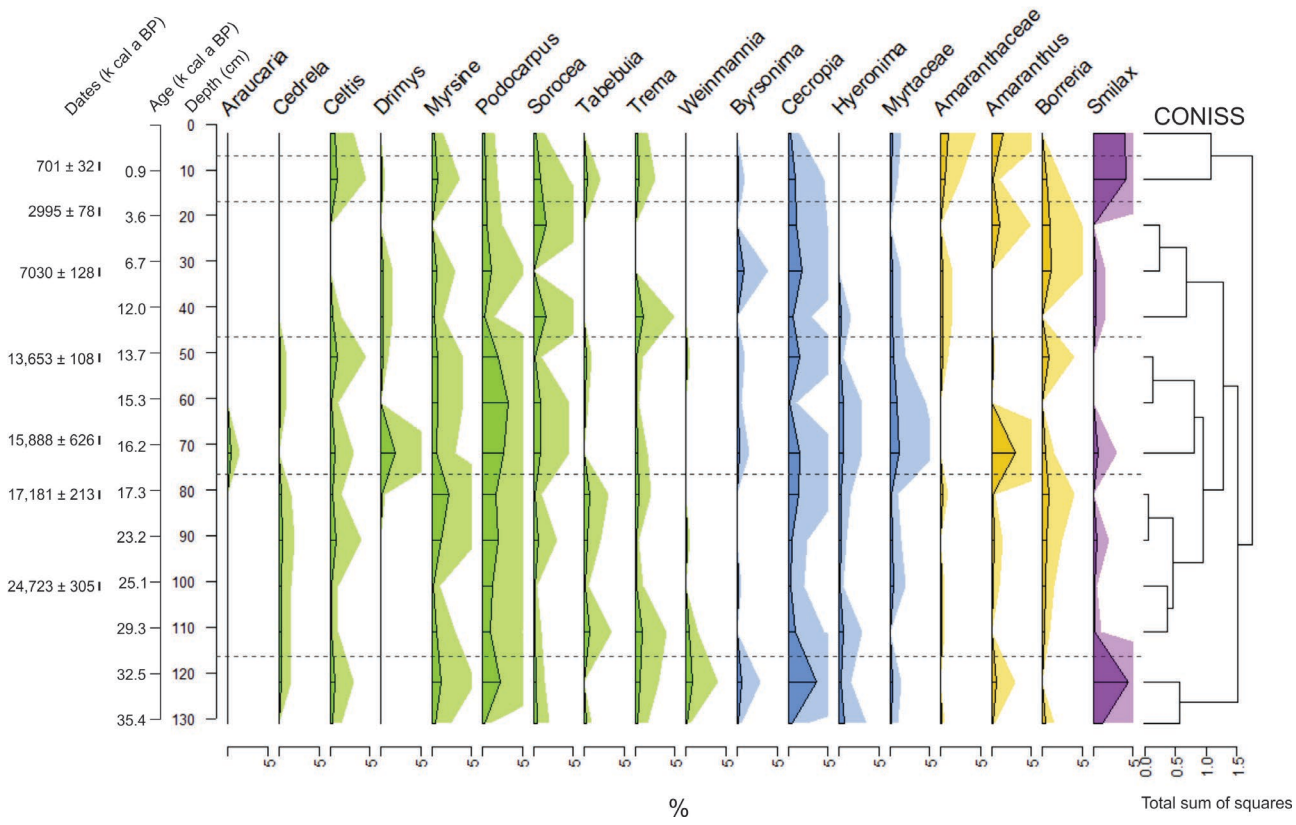
Dates (k cal a BP)
Age (k cal a BP)
Depth (cm)
Araucaria
Cedrela
Celtis
Drimys
Myrsine
Podocarpus
Sorocea
Tabebuia
Trema
Weinmannia
Byrsonima
Cecropia
Hyeronima
Myrtaceae
Amaranthaceae
Amaranthus
Borreria
Smilax
CONISS
701 ± 32
2995 ± 78
7030 ± 128
13,653 ± 108
15,888 ± 626
17,181 ± 213
24,723 ± 305
0.9
3.6
6.7
12.0
13.7
15.3
16.2
17.3
23.2
25.1
29.3
32.5
35.4
0
10
20
30
40
50
60
70
80
90
100
110
120
130
%
Total sum of squares

Figure 6.

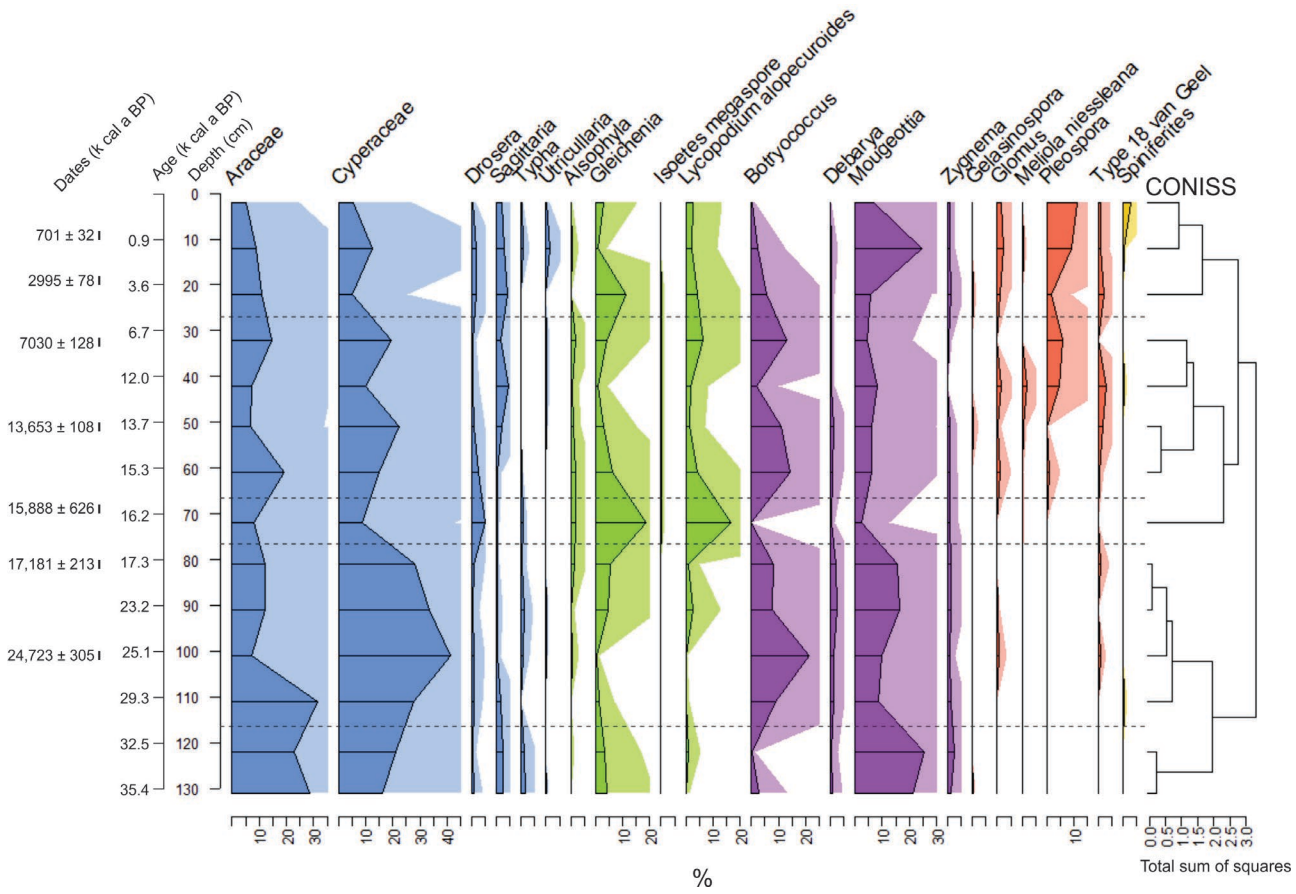
Dates (k cal a BP)
Age (k cal a BP)
Depth (cm)
Araceae
Cyperaceae
Drosera
Sagittaria
Typha
Utricullaria
Alsophyla
Gleichenia
Isoetes megaspore
Lycopodium alopecuroides
Botryococcus
Debarya
Mougeottia
Zygnema
Gelasinospora
Glomus
Meliola niessleana
Pleospora
Type 18 van Geel
Spiniferites
CONISS
701 ± 32
2995 ± 78
7030 ± 128
13,653 ± 108
15,888 ± 626
17,181 ± 213
24,723 ± 305
%
Total sum of squares

Figure 7.

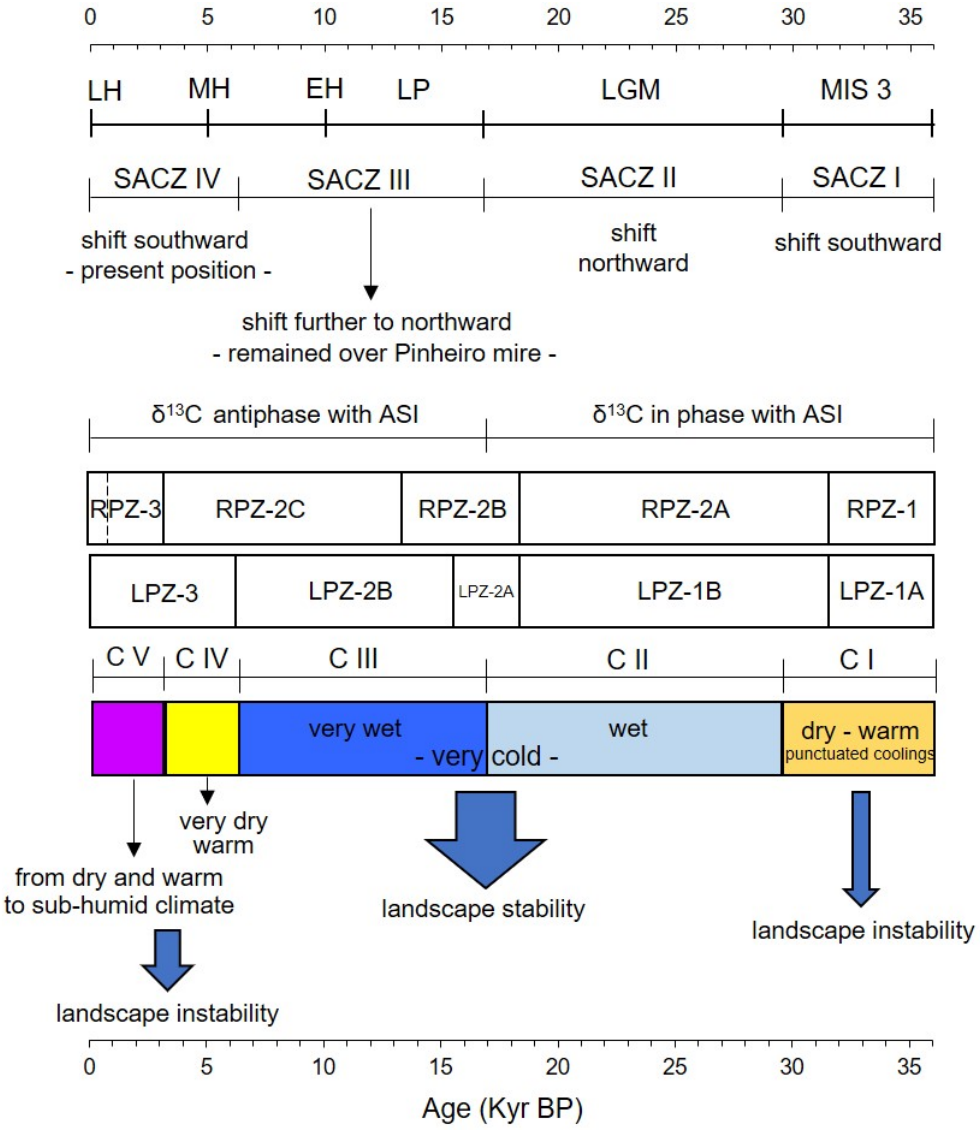
0
5
10
15
20
25
30
35
LH
MH
EH
LP
LGM
MIS 3
SACZ IV
SACZ III
SACZ II
SACZ I
shift southward
- present position -
shift further to northward
- remained over Pinheiro mire -
shift
northward
shift southward
δ13C antiphase with ASI
δ13C in phase with ASI
RPZ-3
RPZ-2C
RPZ-2B
RPZ-2A
RPZ-1
LPZ-3
LPZ-2B
LPZ-2A
LPZ-1B
LPZ-1A
C V
C IV
C III
C II
C I
very wet
- very cold -
wet
dry - warm
punctuated coolings
very dry
warm
from dry and warm
to sub-humid climate
landscape stability
landscape instability
landscape instability
0
5
10
15
20
25
30
35
Age (Kyr BP)

Figure 8.

Late Quaternary vegetation and climate dynamics in central-eastern Brazil: insights from a ~35k cal a BP peat record in the Cerrado biome

INGRID HORÁK-TERRA[1*], ANTONIO MARTÍNEZ CORTIZAS[2], CYNTHIA FERNANDES PINTO DA LUZ[3], ALEXANDRE CHRISTÓFARO SILVA[4], TIM MIGHALL[5], PLÍNIO BARBOSA DE CAMARGO[6], CARLOS VICTOR MENDONÇA-FILHO[7], PAULO EDUARDO DE OLIVEIRA[8], FRANCISCO WILLIAN CRUZ[8], PABLO VIDAL-TORRADO[9]

Supporting Information

Supporting Information document (pp 1-30)

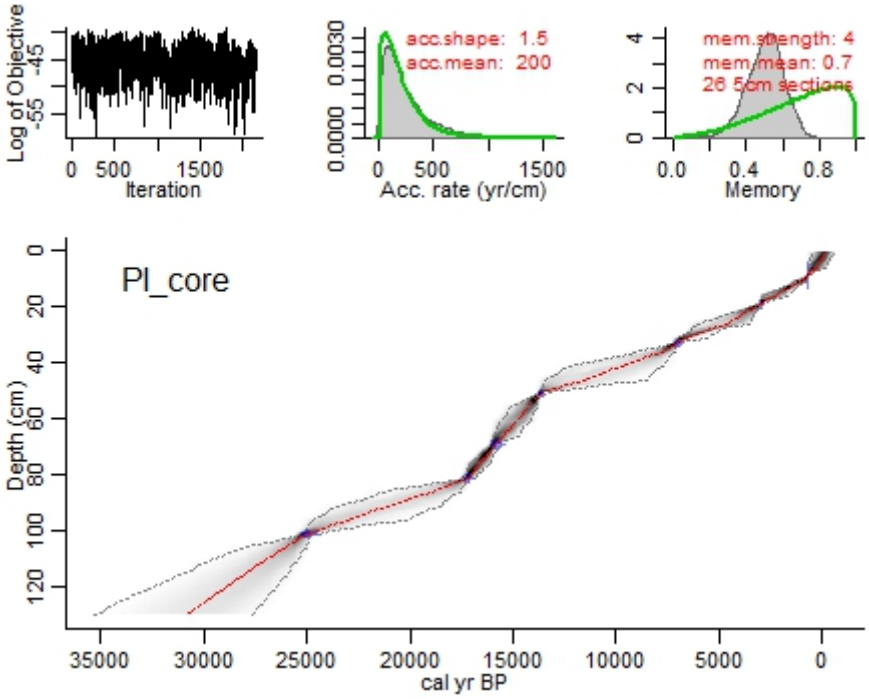

47

48 **Figure S1.** Age-depth model of the PI core fitted with Bacon (Blaauw and Christen, 2011) using the
49 dating for the peat samples of the upper meter of the core (blue) and Northern Hemisphere calibration
50 curve (IntCal13).

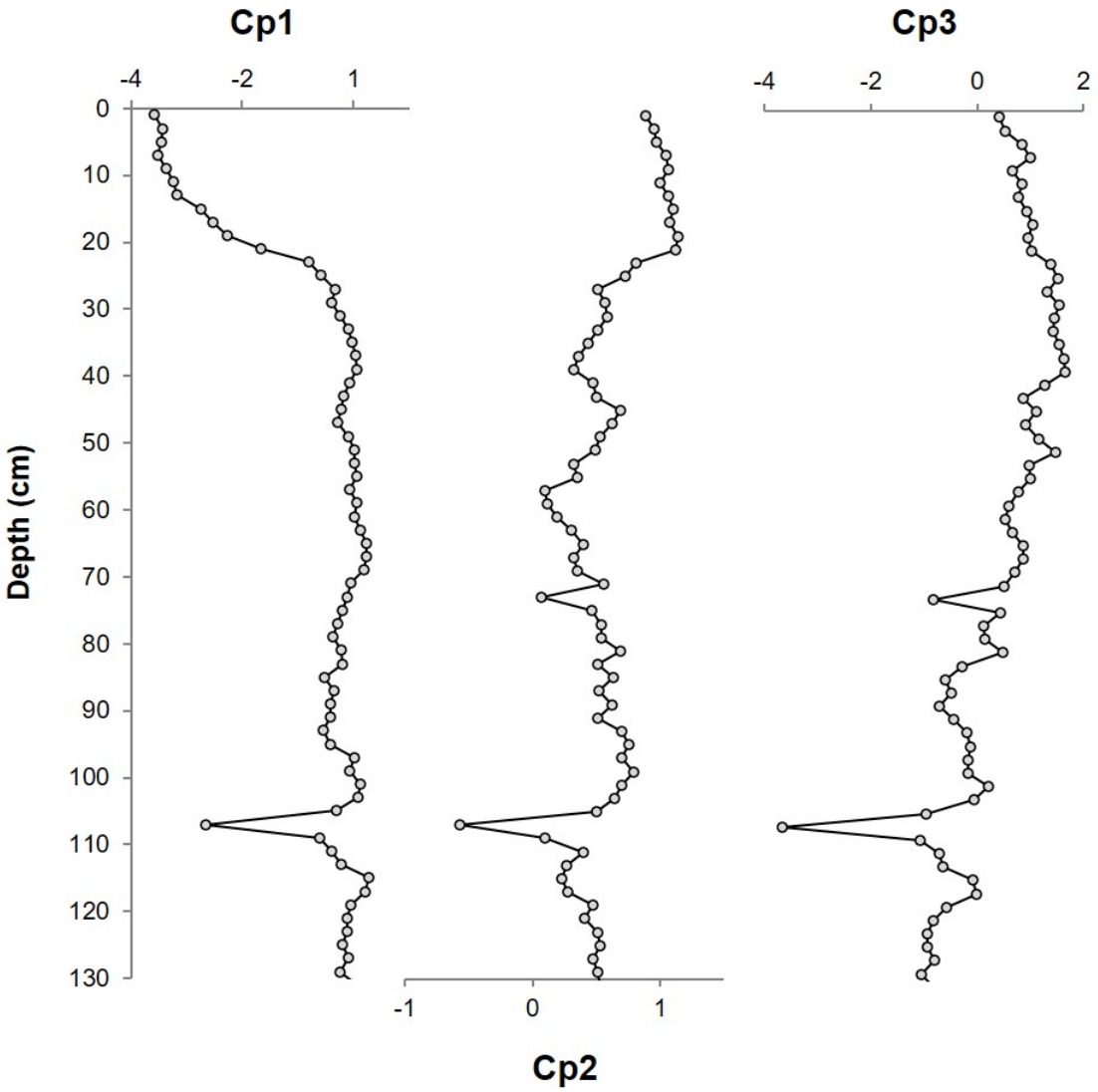

Figure S2. Records of factor scores of the three components of PCA (Cp1, Cp2, and Cp3) for the geochemical composition of the PI core.

	Cp1	Cp2	Cp3
Zr	**0,97**	-0,08	0,02
Y	**0,95**	-0,12	-0,11
Nb	**0,95**	0,08	0,01
Ti	**0,95**	0,21	0,10
Th	**0,91**	-0,06	0,27
Ga	**0,83**	0,36	0,33
Pb	**0,80**	0,49	0,08
Al	**0,79**	-0,30	0,29
Sr	**0,70**	-0,54	0,38
C	0,03	**0,99**	0,00
N	-0,10	**0,98**	0,08
Cr	-0,02	**-0,97**	0,00
Br	0,28	**0,92**	0,13
Si	-0,28	**-0,91**	-0,04
S	-0,26	**0,83**	0,25
K	0,51	**-0,67**	0,42
Fe	0,01	0,24	**0,91**
Rb	0,56	0,02	**0,76**
[1]Eigenv	8.7	6.4	3.0
[2]Var (%)	33.5	24.5	11.6
[3]Var ac	33.5	58.0	69.6

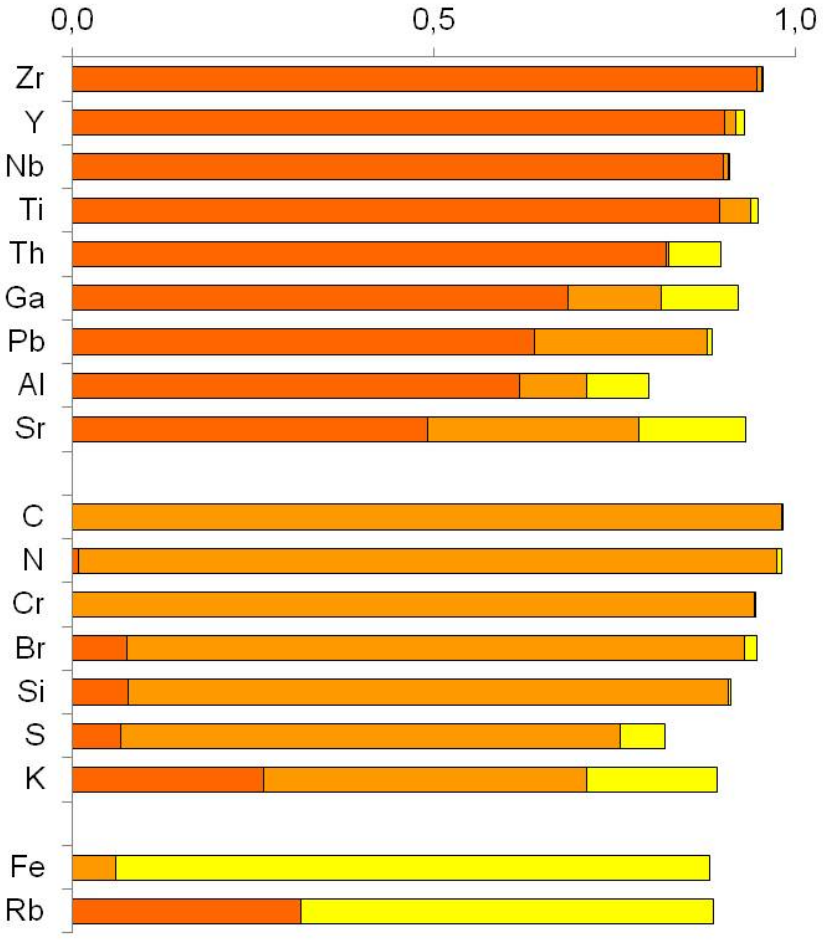

Figure S3. Factor loadings for the three components and fractionation of communalities of the variables used in the PCA of geochemical properties of the PI core. The communality of each variable (i.e. the proportion of its variance explained by each component) corresponds to the total length of the bar; the sections of the bars represent the proportion of variance in each component. The variables are ordered by the component with the largest share of variance. [1]Eigenv: eigenvalues; [2]Var (%): percentage of explained variance; 3Var_ac: cumulative explained variance.

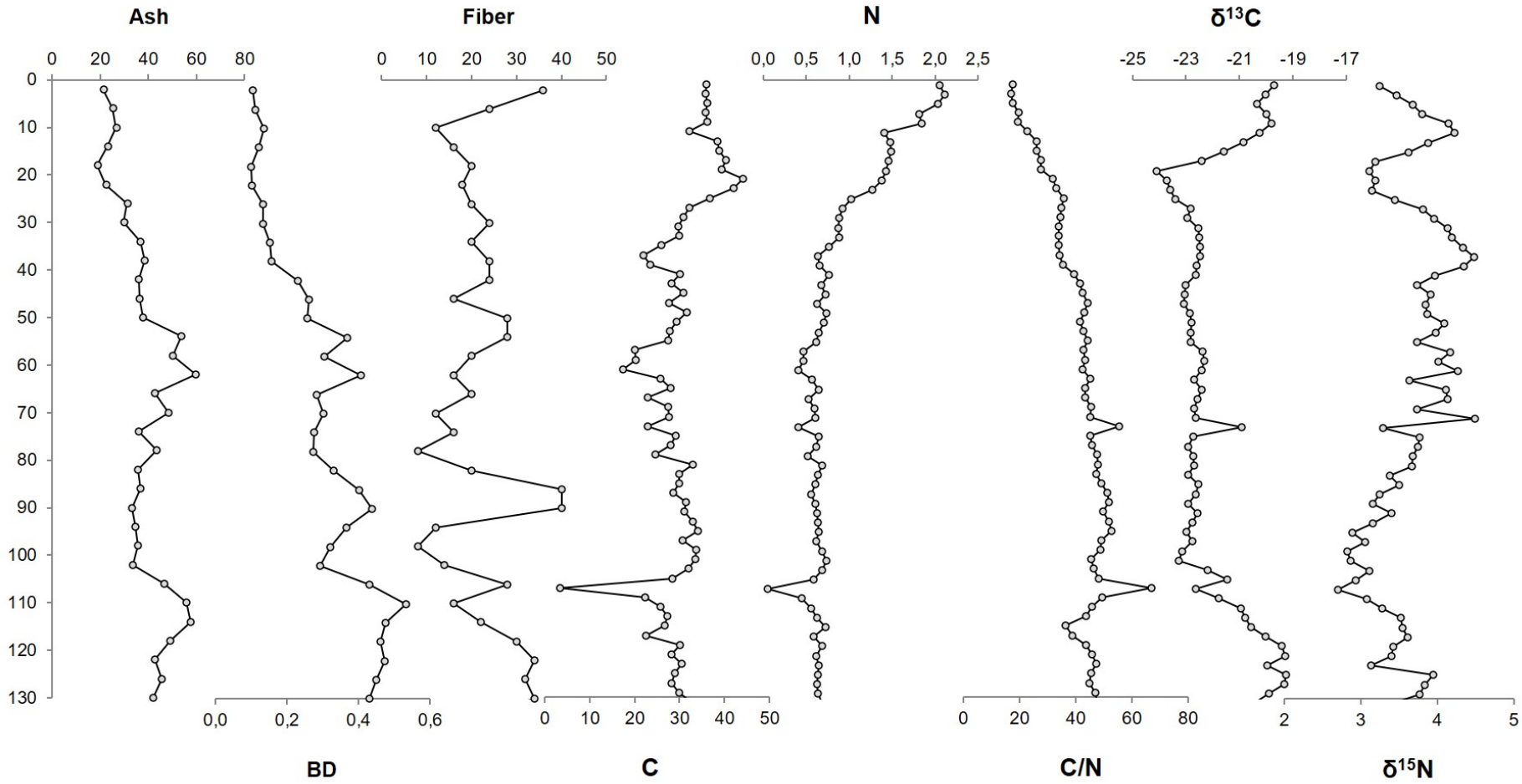

Figure S4. Contents (in %) of ash, fiber, C and N; BD (bulk density; in Mg m^{-3}); and $\delta^{13}C$ and $\delta^{15}N$ (in **‰)** of the PI core.

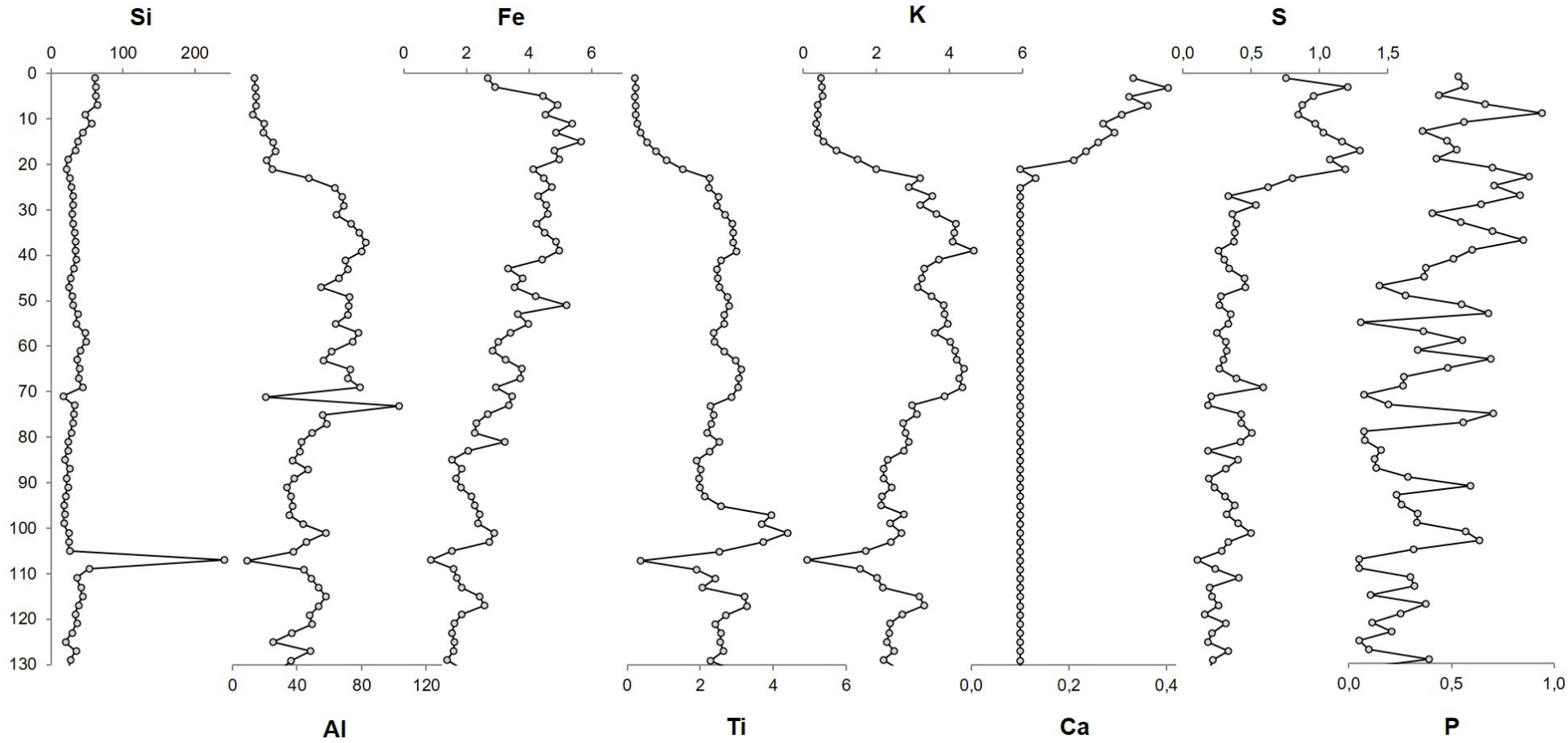

Figure S5. Concentrations (in g kg^{-1}) of Si, Al, Fe, Ti, K, Ca, S, and P of the PI core.

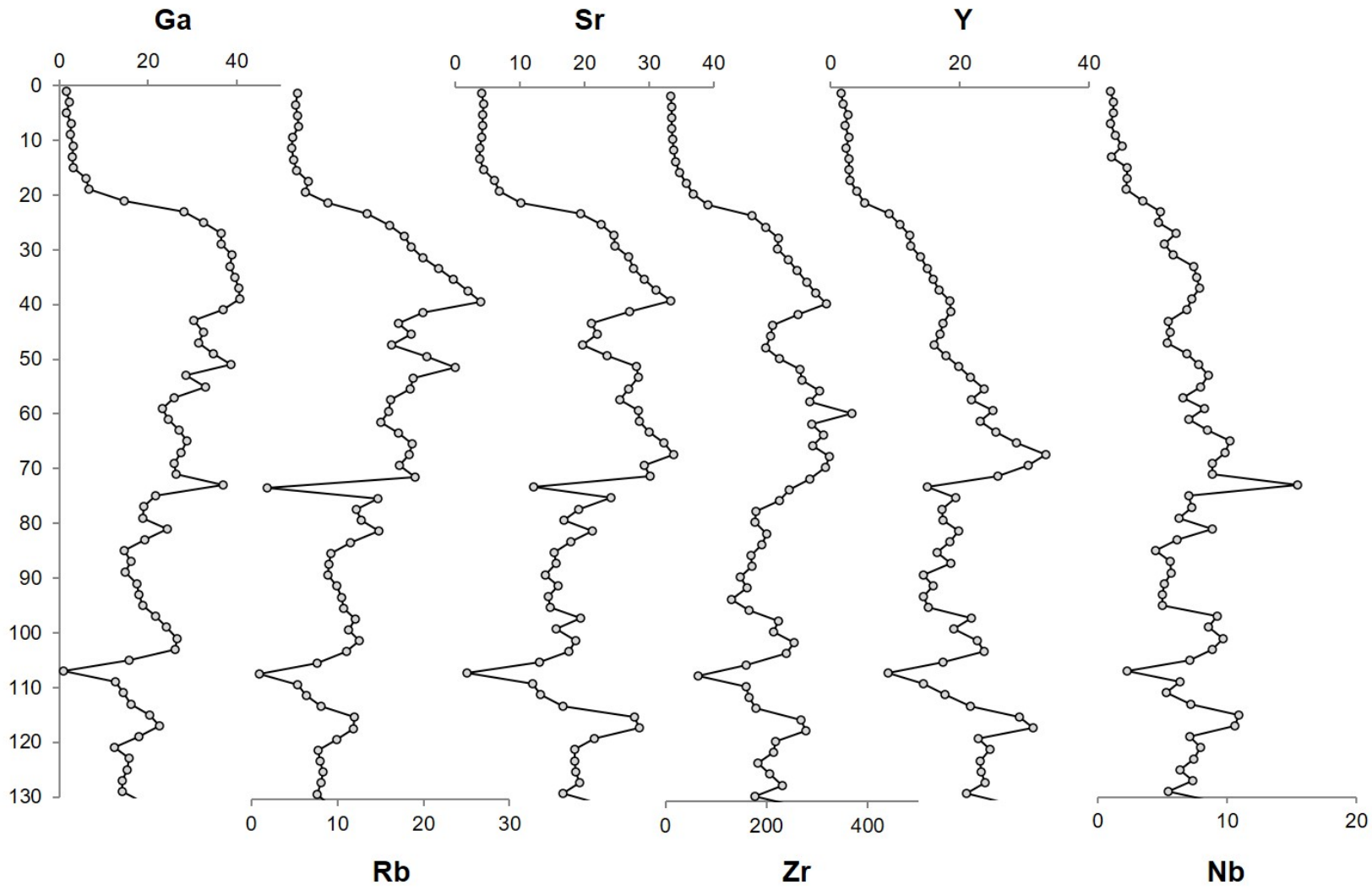

81

82 **Figure S6.** Concentrations (in μg g^{-1}) of Ga, Rb, Sr, Zr, Y, and Nb of the PI core.

83

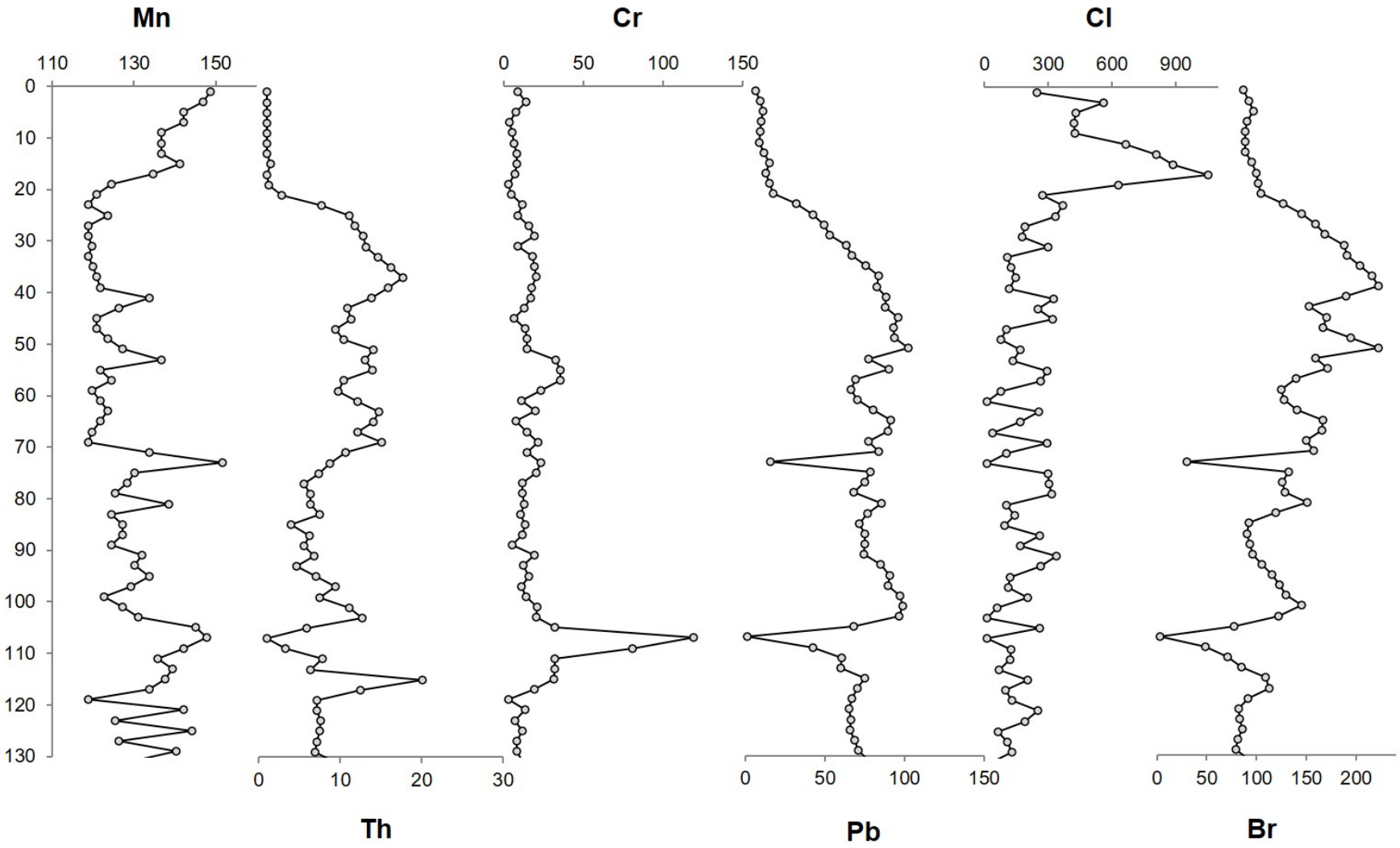

Figure S7. Concentrations (in μg g^{-1}) of Mn, Th, Cr, Pb, Cl, and Br of the PI core.

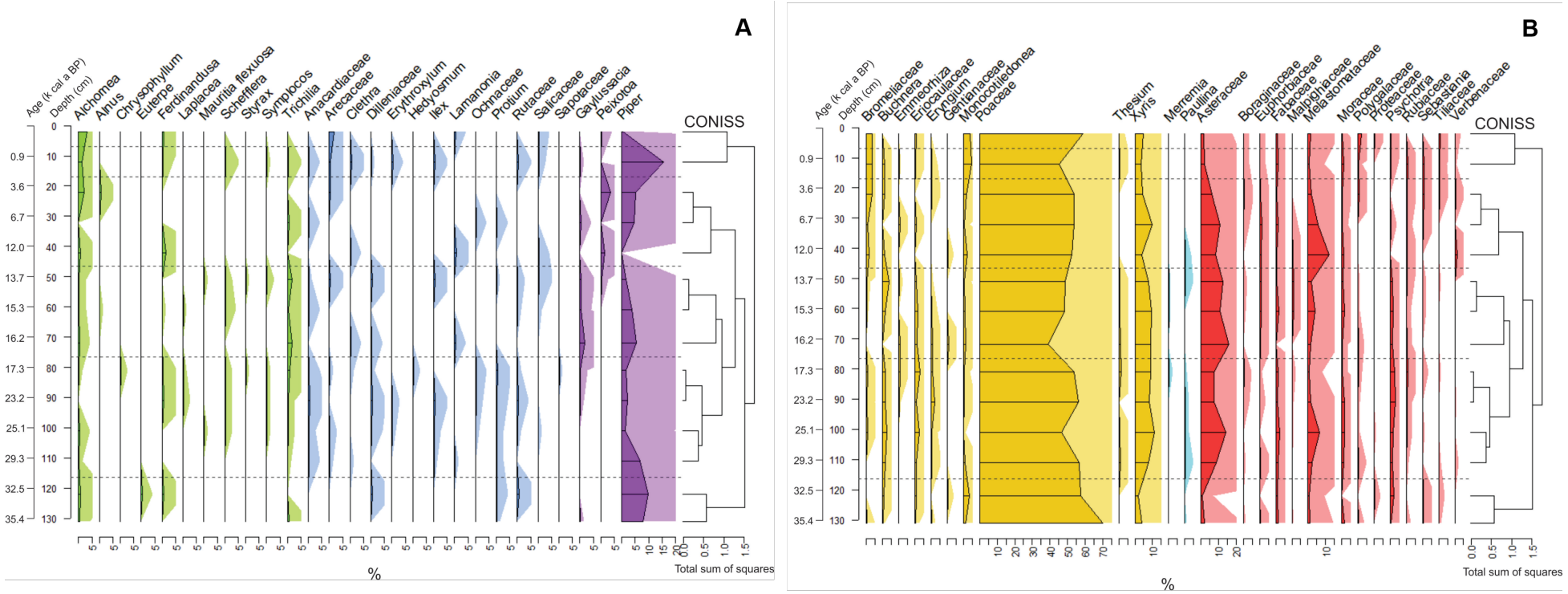

Figure S8. Regional (total land pollen sum) palynological diagram of the PI record with taxa not included in the Figure 6. The silhouettes show the percentage curves of the taxa, while shades show 14x (Figure S8A) and 12x exaggeration curves (Figure S8B). CONISS cluster analysis together with the Regional Palynological Zones (RPZ; separated by dashed lines) are plotted. Values are expressed as percentages of the total land pollen sum (TLP). In Figure S8A: Green: trees; blue: trees/shrubs; and purple: shrubs. In Figure S8B: Yellow: herbs; light blue: lianas; and red: diverses.

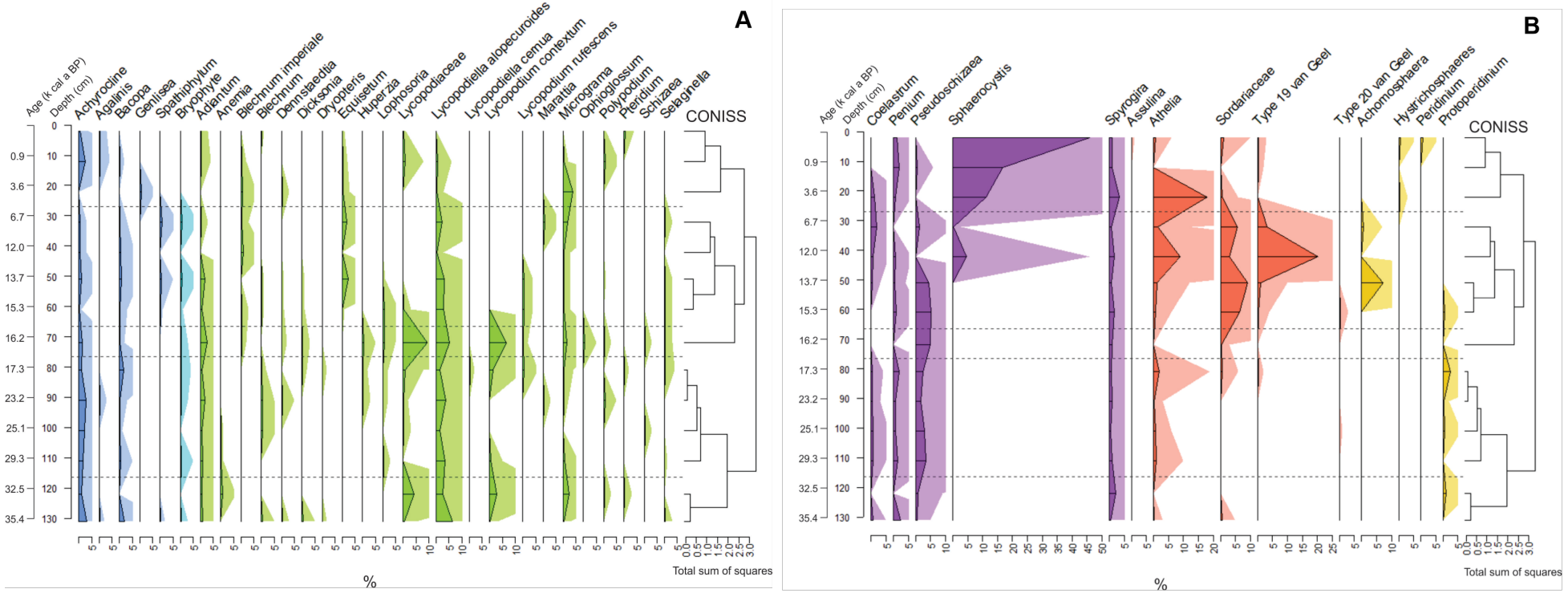

Figure S9. Local (hydro-hygrophytes and NPP) palynological diagram of the PI record with taxa not included in the Figure 7. The silhouettes show the percentage curves of the taxa, while shades show 10x exaggeration curves. CONISS cluster analysis together with the Local Palynological Zones (LPZ; separated by dashed lines) are plotted. Values are expressed as percentages of the total land pollen sum (TLP). In Figure S9A: Blue: hydro-hygrophytes; light blue: bryophyte; and green: pteridophytes. In Figure S9B: Purple: algae; red: fungi; and yellow: dinoflagellates.

Table S1. Results of ^{14}C dating of the PI core, showing conventional age in a BP and calibrated ages (2σ) in cal a BP.

Depth (cm)	[1]Lab. code	Conventional age (a BP)	Calibrated age 2δ (cal a BP)
8-10	Beta - 330480	770 ± 30	701 ± 32
18-20	Beta - 330481	2860 ±30	2995 ± 78
32-34	Beta - 330482	6120±40	7030 ± 128
50-52	Beta - 532630	11,860±40	13,653 ± 108
68-70	Beta - 330483	13,140±60	15,888 ± 626
80-82	Beta - 532631	14,150±40	17,181 ± 213
100-102	Beta - 330484	20,730±100	24,723 ± 305

[1]Beta: Beta Analytic Inc.

Table S2. The maximum number of total land pollen (TLP) and hydro-hygrophytes and non-pollen palynomorphs (NPP) of the PI core.

Depth (cm)	2	12	22	32	42	51	61	72	81	91	101	111	122
TLP	323	1107	191	362	308	1282	931	329	1188	1134	1703	1184	360
hydro-hygrophytes and NPP	674	529	342	301	350	769	698	630	486	647	720	789	352

141 **Table S3**. Pollen and other non-pollen palynomorphs (NPP) observed in PI core, their habit, coverage, and phytophysiognomy belonging or probable
142 environmental indicator.

Pollen, spores and other NPP		Microfossil type	Habit	Coverage*	Phytophysiognomy or environmental indicator**
Genus/Species	**Family**				
Acnistus	Solanaceae	Pollen	Shrubs	R	Semi-deciduous forest
Anadenanthera	Fabaceae	Pollen	Trees	R	Semi-deciduous forest
Apuleia	Fabaceae	Pollen	Trees	R	Semi-deciduous forest
	Aristolochiaceae	Pollen	Lianas/Herbs	R	Semi-deciduous forest
Bathysa	Rubiaceae	Pollen	Trees/Shrubs	R	Semi-deciduous forest
Cedrela	Meliaceae	Pollen	Trees	R	Semi-deciduous forest
Cissus	Vitaceae	Pollen	Lianas/Herbs	R	Semi-deciduous forest
Dennstaedtia	Dennstaedtiaceae	Spore	Arborescent	L	Semi-deciduous forest
Eugenia	Myrtaceae	Pollen	Trees/Shrubs	R	Semi-deciduous forest
Cryptocaria	Lauraceae	Pollen	Trees	R	Semi-deciduous forest
Gaylussacia	Ericaceae	Pollen	Shrubs	R	Semi-deciduous forest
Hedyosmum	Chloranthaceae	Pollen	Trees/Shrubs	R	Semi-deciduous forest
Hyeronima	Euphorbiaceae	Pollen	Trees/Shrubs	R	Semi-deciduous forest

Ilex	Aquifoliaceae	Pollen	Trees/Shrubs	R	Semi-deciduous forest
Jacaranda	Bignoniaceae	Pollen	Trees/Shrubs	R	Semi-deciduous forest
Laplacea	Theaceae	Pollen	Trees	R	Semi-deciduous forest
Lindsaea	Dennstaedtiaceae	Spore	Herbs	L	Semi-deciduous forest
Machaerium	Fabaceae	Pollen	Trees/Shrubs	R	Semi-deciduous forest
Micrograma	Polypodiaceae	Spore	Lianas/Herbs	L	Semi-deciduous forest
Mimosa bimucronata	Fabaceae	Pollen	Trees	R	Semi-deciduous forest
Mikania	Asteraceae	Pollen	Lianas/Herbs	R	Semi-deciduous forest
	Myrtaceae	Pollen	Trees/Shrubs	R	Semi-deciduous forest
Ormosia	Fabaceae	Pollen	Trees	R	Semi-deciduous forest
Paullinia	Sapindaceae	Pollen	Lianas	R	Semi-deciduous forest
Piptadenia	Fabaceae	Pollen	Trees	R	Semi-deciduous forest
Protium	Burseraceae	Pollen	Trees/Shrubs	R	Semi-deciduous forest
	Salicaceae	Pollen	Trees/Shrubs	R	Semi-deciduous forest
Siphoneugena	Myrtaceae	Pollen	Trees/Shrubs	R	Semi-deciduous forest
Sloanea	Elaeocarpaceae	Pollen	Herbs	R	Semi-deciduous forest
Sorocea	Moraceae	Pollen	Trees	R	Semi-deciduous forest

Spathiphyllum	Araceae	Pollen	Herbs	L	Semi-deciduous forest
Alnus	Betulaceae	Pollen	Trees	R	Cold and humid forest
Alsophila	Geometridae	Spore	Arborescent	L	Cold and humid forest
Araucaria	Araucariaceae	Pollen	Trees	R	Cold and humid forest
Dicksonia	Dicksoniaceae	Spore	Arborescent	L	Cold and humid forest
Drimys	Winteraceae	Pollen	Trees	R	Cold and humid forest
Hypolepis	Dennstaedtiaceae	Spore	Herbs/Shrubs	L	Cold and humid forest
Lophosoria	Dicksoniacea	Spore	Arborescent	L	Cold and humid forest
Myrsine	Myrsinaceae	Pollen	Trees	R	Cold and humid forest
Podocarpus	Podocarpaceae	Pollen	Trees	R	Cold and humid forest
Rhamnus	Rhamnaceae	Pollen	Trees/Shrubs	R	Cold and humid forest
Trichilia	Meliaceae	Pollen	Trees	R	Cold and humid forest
Clethra	Clethraceae	Pollen	Trees/Shrubs	R	Mountain forest
Galium	Rubiaceae	Pollen	Herbs	R	Mountain forest
Huperzia	Lycopodiaceae	Spore	Herbs	L	Mountain forest
Lamanonia	Cunnoniaceae	Pollen	Trees/Shrubs	R	Mountain forest
Marattia	Marattiaceae	Spore	Arborescent	R	Mountain forest

Mimosa scabrella	Fabaceae	Pollen	Trees	R	Mountain forest
Acacia	Fabaceae	Pollen	Diverses	R	Savanna forest
Aegiphila	Verbenaceae	Pollen	Trees/Shrubs	R	Savanna forest
	Anacardiaceae	Pollen	Trees/Shrubs	R	Savanna forest
Cabralea	Meliaceae	Pollen	Trees/Shrubs	R	Savanna forest
Casearia	Fabaceae	Pollen	Trees/Shrubs	R	Savanna forest
Chrysophyllum	Sapotaceae	Pollen	Trees	R	Savanna forest
Copaifera	Fabaceae	Pollen	Trees/Shrubs	R	Savanna forest
Luehea	Tiliaceae	Pollen	Trees	R	Savanna forest
Matayba	Sapindaceae	Pollen	Trees/Shrubs	R	Savanna forest
	Ochnaceae	Pollen	Trees/Shrubs	R	Savanna forest
Prestonia	Apocynaceae	Pollen	Lianas/Herbs	R	Savanna forest
	Sapotaceae	Pollen	Trees/Shrubs	R	Savanna forest
Schinus	Anacardiaceae	Pollen	Trees/Shrubs	R	Savanna forest
Senna	Fabaceae	Pollen	Trees/Shrubs	R	Savanna forest
Smilax	Smilacaceae	Pollen	Lianas	R	Savanna forest
Struthanthus	Loranthaceae	Pollen	Lianas/Herbs	R	Savanna forest

Tabebuia rosea	Bignoniaceae	Pollen	Trees	R	Savanna forest
Tabebuia	Bignoniaceae	Pollen	Trees	R	Savanna forest
Vitex	Verbenaceae	Pollen	Trees/Shrubs	R	Savanna forest
Zanthoxylum	Rutaceae	Pollen	Trees	R	Savanna forest
	Arecaceae	Pollen	Trees/Shrubs	R	Humid savanna
Alchornea	Euphorbiaceae	Pollen	Trees	R	Humid savanna
Astronium	Anacardiaceae	Pollen	Trees	R	Humid savanna
Calyptranthes	Myrtaceae	Pollen	Trees	R	Humid savanna
Chelonanthus	Gentianaceae	Pollen	Shrubs	R	Humid savanna
Davilla	Dilleniaceae	Pollen	Lianas	R	Humid savanna
Diodia	Rubiaceae	Pollen	Herbs/Shrubs	R	Humid savanna
Euterpe	Arecaceae	Pollen	Trees	R	Humid savanna
Ferdinandusa	Rubiaceae	Pollen	Trees	R	Humid savanna
Genipa	Rubiaceae	Pollen	Trees	R	Humid savanna
Mascagnia	Malpighiaceae	Pollen	Lianas	R	Humid savanna
Mauritia flexuosa	Arecaceae	Pollen	Trees	R	Humid savanna
	Menispermaceae	Pollen	Lianas	R	Humid savanna

Myrcia	Myrtaceae	Pollen	Trees/Shrubs	R	Humid savanna
Platymiscium	Fabaceae	Pollen	Trees	R	Humid savanna
Schefflera	Araliaceae	Pollen	Trees	R	Humid savanna
Styrax	Styracaceae	Pollen	Trees	R	Humid savanna
Symplocos	Symplocaceae	Pollen	Trees	R	Humid savanna
Trixis	Asteraceae	Pollen	Herbs/Shrubs	R	Humid savanna
Andira	Fabaceae	Pollen	Trees/Shrubs	R	Dry savanna
Byrsonima	Malpighiaceae	Pollen	Trees/Shrubs	R	Dry savanna
Cassia	Fabaceae	Pollen	Diverses	R	Dry savanna
Croton	Euphorbiaceae	Pollen	Herbs/Shrubs	R	Dry savanna
Hortia	Rutaceae	Pollen	Shrubs	R	Dry savanna
Mimosa	Fabaceae	Pollen	Diverses	R	Dry savanna
	Proteaceae	Pollen	Trees/Shrubs	R	Dry savanna
Roupala	Proteaceae	Pollen	Trees/Shrubs	R	Dry savanna
Serjania	Sapindaceae	Pollen	Lianas	R	Dry savanna
Banara	Salicaceae	Pollen	Shrubs	R	Pioneer of secondary forest
Cecropia	Urticaceae	Pollen	Trees/Shrubs	R	Pioneer of secondary forest

Doliocarpus	Dilleniaceae	Pollen	Lianas	R	Pioneer of secondary forest
Erythroxylum	Erythroxylaceae	Pollen	Trees/Shrubs	R	Pioneer of secondary forest
Inga	Fabaceae	Pollen	Trees	R	Pioneer of secondary forest
Piper	Piperaceae	Pollen	Shrubs	R	Pioneer of secondary forest
Tapirira	Anacardiaceae	Pollen	Trees/Shrubs	R	Pioneer of secondary forest
Cestrum	Solanaceae	Pollen	Shrubs	R	Savanna abroad sense
Chamaecrista	Fabaceae	Pollen	Diverses	R	Savanna abroad sense
Clitoria	Fabaceae	Pollen	Diverses	R	Savanna abroad sense
Cordia	Boraginaceae	Pollen	Trees/Shrubs	R	Savanna abroad sense
Cupania	Sapindaceae	Pollen	Trees/Shrubs	R	Savanna abroad sense
Dasyphyllum	Asteraceae	Pollen	Trees/Shrubs	R	Savanna abroad sense
Eupatorium	Asteraceae	Pollen	Herbs/Shrubs	R	Savanna abroad sense
Guettarda	Rubiaceae	Pollen	Trees/Shrubs	R	Savanna abroad sense
Hyptis	Lamiaceae	Pollen	Herbs/Shrubs	R	Savanna abroad sense
Laetia	Salicaceae	Pollen	Shrubs	R	Savanna abroad sense
Lantana	Verbenaceae	Pollen	Herbs/Shrubs	R	Savanna abroad sense
Merremia	Convolvulaceae	Pollen	Lianas	R	Savanna abroad sense

Peixotoa	Malpighiaceae	Pollen	Shrubs	R	Savanna abroad sense
Periandra	Fabaceae	Pollen	Lianas	R	Savanna abroad sense
Psidium	Myrtaceae	Pollen	Trees/Shrubs	R	Savanna abroad sense
Rudgea	Rubiaceae	Pollen	Diverses	R	Savanna abroad sense
Sebastiania	Euphorbiaceae	Pollen	Diverses	R	Savanna abroad sense
Solanum	Solanaceae	Pollen	Diverses	R	Savanna abroad sense
Strychnos	Loganiaceae	Pollen	Diverses	R	Savanna abroad sense
Tetrapterys	Malpighiaceae	Pollen	Diverses	R	Savanna abroad sense
	Verbenaceae	Pollen	Diverses	R	Savanna abroad sense
Agalinis	Orobanchaceae	Pollen	Herbs	L	Wet grassland
Baccharis	Asteraceae	Pollen	Herbs/Shrubs	R	Wet grassland
Bacopa	Orobanchaceae	Pollen	Herbs	L	Wet grassland
Begonia	Begoniaceae	Pollen	Herbs	R	Wet grassland
Bidens	Asteraceae	Pollen	Herbs/Shrubs	R	Wet grassland
Campylopodium	Dicranaceae	Moss	Herbs	L	Wet grassland
Campylopus	Dicranaceae	Moss	Herbs	L	Wet grassland
Dicranella	Dicranaceae	Moss	Herbs	L	Wet grassland

Drosera	Droseraceae	Pollen	Herbs	L	Wet grassland
Eryngium	Apiaceae	Pollen	Herbs	R	Wet grassland
Genlisea	Lentibulariaceae	Pollen	Herbs	L	Wet grassland
Gnaphalium	Asteraceae	Pollen	Herbs	R	Wet grassland
Heliotropium	Boraginaceae	Pollen	Herbs	R	Wet grassland
Hydrocotyle	Apiaceae	Pollen	Herbs	L	Wet grassland
Ichthyothere/Aspilia	Asteraceae	Pollen	Herbs/Shrubs	R	Wet grassland
Myriophyllum	Haloragaceae	Pollen	Herbs	L	Wet grassland
	Nymphaeaceae/Pontederiaceae	Pollen	Herbs	L	Wet grassland
Nymphoides	Menyanthaceae	Pollen	Herbs	L	Wet grassland
	Orobanchaceae	Pollen	Herbs/Shrubs	R	Wet grassland
Phaeoceros	Anthocerotaceae	Moss	Herbs	L	Wet grassland
Sagittaria	Alismataceae	Pollen	Herbs	L	Wet grassland
Sphagnum recurvum	Sphagnaceae	Moss	Herbs	L	Wet grassland
Typha	Typhaceae	Pollen	Herbs	L	Wet grassland
Utricularia	Lentibulariaceae	Pollen	Herbs	L	Wet grassland
Acalypha	Euphorbiaceae	Pollen	Herbs/Shrubs	R	Dry grassland

Achyrocline	Asteraceae	Pollen	Herbs	L	Dry grassland
Amaranthus	Amaranthaceae	Pollen	Herbs	R	Dry grassland
Anemia	Schizaeaceae	Spore	Herbs	L	Dry grassland
Borreria	Rubiaceae	Pollen	Herbs	R	Dry grassland
Camarea	Maplpighiaceae	Pollen	Herbs/Shrubs	R	Dry grassland
Cleome	Capparaceae	Pollen	Herbs/Shrubs	R	Dry grassland
Chamaesyce	Euphorbiaceae	Pollen	Herbs	R	Dry grassland
Ephedra	Ephedraceae	Pollen	Schrubs	R	Dry grassland
Eremanthus	Asteraceae	Pollen	Diverses	R	Dry grassland
Euphorbia	Euphorbiaceae	Pollen	Herbs	R	Dry grassland
Galactia	Fabaceae	Pollen	Herbs	R	Dry grassland
Gleichenia 1	Gleicheniaceae	Spore	Shrubs	L	Dry grassland
Gleichenia 2	Gleicheniaceae	Spore	Shrubs	L	Dry grassland
Phytolacca	Phytolaccaceae	Pollen	Herbs	R	Dry grassland
	Polygalaceae	Pollen	Diverses	R	Dry grassland
Scoparia	Orobanchaceae	Pollen	Herbs	R	Dry grassland
Senecio	Asteraceae	Pollen	Herbs/Shrubs	R	Dry grassland

Zornia	Fabaceae	Pollen	Diverses	R	Dry grassland
	Bromeliaceae	Pollen	Herbs	R	Rupicola-saxicolous grassland
Coccocypselum/Declieuxia	Rubiaceae	Pollen	Herbs/Shrubs	R	Rupicola-saxicolous grassland
Cuphea	Lythraceae	Pollen	Herbs/Shrubs	R	Rupicola-saxicolous grassland
	Eriocaulaceae	Pollen	Herbs	R	Rupicola-saxicolous grassland
Xyris	Xyridaceae	Pollen	Herbs	R	Rupicola-saxicolous grassland
Alternanthera	Amaranthaceae	Pollen	Herbs	R	Grassland
	Araceae	Pollen	Herbs	L	Grassland
Buchnera	Orobanchaceae	Pollen	Herbs	R	Grassland
	Campanulaceae	Pollen	Herbs/Shrubs	R	Grassland
Cassytha	Lauraceae	Pollen	Herbs	R	Grassland
Crotalaria	Fabaceae	Pollen	Herbs/Shrubs	R	Grassland
	Cyperaceae	Pollen	Herbs	L	Grassland
Gomphrena	Amaranthaceae	Pollen	Herbs	R	Grassland
	Iridaceae	Pollen	Herbs	R	Grassland
	Monocotiledonea	Pollen	Herbs	R	Grassland
	Poaceae	Pollen	Herbs	R	Grassland

Thesium	Santalaceae	Pollen	Herbs	R	Grassland
	Apocynaceae	Pollen	Diverses	R	Diverse
	Bignoniaceae	Pollen	Diverses	R	Diverse
	Euphorbiaceae	Pollen	Diverses	R	Diverse
	Fabaceae	Pollen	Diverses	R	Diverse
Justicia	Acanthaceae	Pollen	Herbs/Shrubs	R	Diverse
	Lauraceae	Pollen	Diverses	R	Diverse
	Lythraceae	Pollen	Diverses	R	Diverse
	Malpighiaceae	Pollen	Diverses	R	Diverse
	Malvaceae	Pollen	Herbs/Shrubs	R	Diverse
	Melastomataceae	Pollen	Diverses	R	Diverse
Phyllanthus	Euphorbiaceae	Pollen	Herbs/Shrubs	R	Diverse
Polypodium	Polypodiaceae	Spore	Herbs	R	Diverse
Psychotria	Rubiaceae	Pollen	Diverses	R	Diverse
	Rubiaceae	Pollen	Diverses	R	Diverse
	Solanaceae	Pollen	Diverses	R	Diverse
Schizaea	Schizaeaceae	Spore	Herbs	L	Diverse

Selaginella	Selaginellaceae	Spore	Lianas/Herbs	L	Diverse
	Tiliaceae	Pollen	Diverses	R	Diverse
Vernonia	Asteraceae	Pollen	Herbs/Shrubs	R	Diverse
Vigna	Fabaceae	Pollen	Lianas	R	Diverse
Equisetum	Equisetaceae	Spore	Herbs/Shrubs	L	Humid forest and wet grassland
Lycopodiella alopecuroides	Lycopodiaceae	Spore	Herbs	L	Humid forest and wet grassland
Lycopodiella cernua	Lycopodiaceae	Spore	Herbs	L	Humid forest and wet grassland
Lycopodium contextum	Lycopodiaceae	Spore	Herbs	L	Humid forest and wet grassland
Lycopodium rufescens	Lycopodiaceae	Spore	Herbs	L	Humid forest and wet grassland
Osmunda	Osmundaceae	Spore	Herbs	L	Humid forest and wet grassland
Ophioglossum	Ophioglossaceae	Spore	Herbs	L	Humid forest and wet grassland
Adiantum	Pteridaceae	Spore	Herbs	L	Forest
	Moraceae	Pollen	Diverses	R	Forest
Pleopeltis	Polypodiaceae	Spore	Herbs	L	Forest

Thunbergia	Acanthaceae	Pollen	Lianas	R	Forest
Blechnum imperiale	Blechnaceae	Spore	Herbs	L	Soil erosion
Blechnum	Blechnaceae	Spore	Herbs	L	Soil erosion
Glomus	Glomeraceae	Fungi		L	Soil erosion
Pseudoschizaea		Algae		L	Soil erosion
Achomosphaera	Hystrichosphaeraceae	Pyrrophyta		L	Warm waters
	Dinophyceae	Pyrrophyta		L	Warm waters
Lingulodinium	Gonyaulacaceae	Pyrrophyta		L	Warm waters
Spiniferites	Gonyaulacaceae	Pyrrophyta		L	Warm waters
Delitschia	Delitschiaceae	Fungi		L	Coprophilous fungi
	Sordariaceae	Fungi		L	Coprophilous fungi
Type 19 van Geel		Fungi		L	Coprophilous fungi
Dryopteris	Dryopteridaceae	Spore	Lianas/Shrubs	L	Landscape disturbance
Hystrichosphaeres	Dinophyceae	Pyrrophyta		L	Landscape disturbance
	Lycopodiaceae	Spore	Herbs/Shrubs	L	Landscape disturbance
Pteridium	Dennstaedtiaceae	Spore	Herbs	L	Landscape disturbance
Coelastrum	Scenedesmaceae	Algae		L	Water quality

Euastrum	Desmidiaceae	Algae	L	Water quality
Penium	Peniaceae	Algae	L	Water quality
Sphaerocystis 1	Palmellaceae	Algae	L	Water quality
Sphaerocystis 2	Palmellaceae	Algae	L	Water quality
Botryococcus	Dictyosphaeriaceae	Algae	L	Changes in hydrology
Spyrogira	Zygnemataceae	Algae	L	Changes in hydrology
Type 718 van Geel		Palynomorph	L	Changes in hydrology
Type 726 van Geel		Palynomorph	L	Changes in hydrology
Assulina	Euglyphidae	Fungi	L	Wet conditions
Meliola niessleana	Melanconidaceae	Fungi	L	Wet conditions
Type 18 van Geel		Fungi	L	Wet conditions
Type 140 van Geel		Fungi	L	Wet conditions
Type 731 van Geel		Palynomorph	L	Wet conditions
Gelasinospora	Sordariaceae	Fungi	L	Dry conditions
Pleospora	Pleosporaceae	Fungi	L	Dry conditions
Type 20 van Geel		Fungi	L	Dry conditions
Type 37 van Geel		Rotifers	L	Dry conditions

Isoetes Megaspore	Isoetaceae	Spore	Herbs	L	Permanent flooding
Type 121 van Geel		Fungi		L	Permanent flooding
Mougeotia	Zygnemataceae	Algae		L	Shallow open water
Zygnema	Zygnemataceae	Algae		L	Shallow open water
Debarya	Zygnemataceae	Algae		L	Airbone/lower temperature
Athelia	Corticiaceae	Fungi		L	Parasite on woody substrates
Dictyosporites sp.	Dictyosporae	Fungi		L	Parasite on woody substrates
Type 12 van Geel		Fungi		L	Cellulose decomposed
Peridinium	Podolampaceae	Pyrrophyta		L	Bloom's collapse post
Protoperidinium	Podolampaceae	Pyrrophyta		L	Paleoproductivity
Type 719 van Geel		Palynomorph		L	Moss samples

*L: Local; R: Regional. **References: Ellis and van Geel (1978); Guy-Ohlson (1992); Kołaczek et al. (2012); Marchant et al. (2002); Mendonça et al. (1998); Nobel (1978); Sánchez-González et al. (2010); Sehnem (1970); van Geel (1976); van Geel (1978); van Geel and Aptroot (2006); van Geel et al. (1989); van Geel and Middeldorp (1988).

References

Blaauw M, Christen JA. 2011. Flexible paleoclimate age-depth models using an autoregressive gamma process. *Bayesian Analysis* **6**: 457–474, https://doi.org/10.1214/11-BA618

Ellis AAC, van Geel B. 1978. Fossil zygospores of Debarya glyptosprema (De Bary) Wittr. (Zygnemataceae) in Holocene sandy soils. *Acta Botanica Neerlandica* **27**: 389-396, https://doi.org/10.1111/j.1438-8677.1978.tb00308.x

Guy-Ohlson D. 1992. Botryococcus as an aid in the interpretation of palaeoenvironment and depositional processes. *Review of Palaeobotany and Palynology* **71**: 1–15, https://doi.org/10.1016/0034-6667(92)90155-A

Kołaczek P, Karpińska-Kołaczek M, Worobiec E, *et al*. 2012. *Debarya glyptosperma* (De Bary) Wittrock 1872 (Zygnemataceae, Chlorophyta) as a possible airborne alga – a contribution to its palaeoecological interpretation. *Acta Palaeobotanica* **521**: 139–146.

Marchant R, Almeida L, Behling H, *et al*. 2002. Distribution and ecology of parent taxa of pollen lodged within the Latin America Pollen Database. *Review of Palaeobotany and Palynology* **121:** 1-75, https://doi.org/10.1016/S0034-6667(02)00082-9

Mendonça RC, Felfili JM, Walter BMT, *et al*. 1998. Flora vascular do cerrado. In *Cerrado: ambiente e flora,* Sano SM, Almeida SP (eds). Embrapa: Brazil; 289-556.

Nobel PS. 1978. Microhabitat, water relations, and photosynthesis of a desert fern, *Notholaena parryi*. *Oecologia* **31**: 293-309, https://doi.org/10.1007/BF00346249

Sánchez-González A, Zúñiga EA, Tejero-Díez JD. 2010. Richness and distribution patterns of ferns and lycopods in Los Mármoles National Park, Hidalgo, Mexico. *The Journal of the* Torrey *Botanical* Society **137**: 373-379, https://doi.org/10.3159/10-RA-002.1

Sehnem A. 1970. Polipodiáceas. In *Flora Ilustrada Catarinense,* Reitz R (ed). Herbário Barbosa Rodrigues: Brazi; 1-173.

van Geel BA. 1976. A paleoecological study of Holocene peat bog sections, based on the analysis of pollen, spores and macro and microscopic remains of fungi, algae, cormophytes and animals. Doctoral thesis. *Universiteit van Amsterdam*.

van Geel BA. 1978. A palaeoecological study of holocene peat bog sections in Germany and The Netherlands, based on the analysis of pollen, spores and macro- and microscopic remains of fungi, algae, cormophytes and animals. *Review of Palaeobotany and Palynology* **25**: 1-120, https://doi.org/10.1016/0034-6667(78)90040-4

van Geel B, Middeldorp AA. 1988. Vegetational history of Carbury Bog (Co. Kildare, Ireland) during the last 850 years and a test of the temperature indicator value of 2H/1H measurements of peat samples in relation to historical sources and meteorological data. *New Phytologist* **109**: 377-392, https://doi.org/10.1111/j.1469-8137.1988.tb04208.x

van Geel B, Coope GR, van Der Hammen T. 1989. Palaeoecology and stratigraphy of the Late-glacial type section at Usselo (The Netherlands). *Review of Palaeobotany and Palynology* **60**: 25-129, https://doi.org/10.1016/0034-6667(89)90072-9

van Geel B, Aproot A. 2006. Fossil ascomycetes in Quaternary deposits. *Nova Hedwigia* **82**: 313-329, https://doi.org/10.1127/0029-5035/2006/0082-0313